5.1 Introduction

The ubiquity of sulfonamides in pharmaceutical and agricultural products is impressive for a functional group rarely encountered in nature. A growing number of modern bioactive compounds are designed with the sulfonamide functional group (2016 saw 15% of the top 100 prescription medications be sulfonamides) because of its heteroatom composition, three-dimensional structure, favorable physiochemical properties, chemical and metabolic stability, and frequent crystalline form. Sulfonamide synthesis via sulfonylation has sparked significant interest from both academic research institutions and commercial manufacturers owing to its exceptional efficiency in sulfonamide production (Figure 5.1) [1-8].

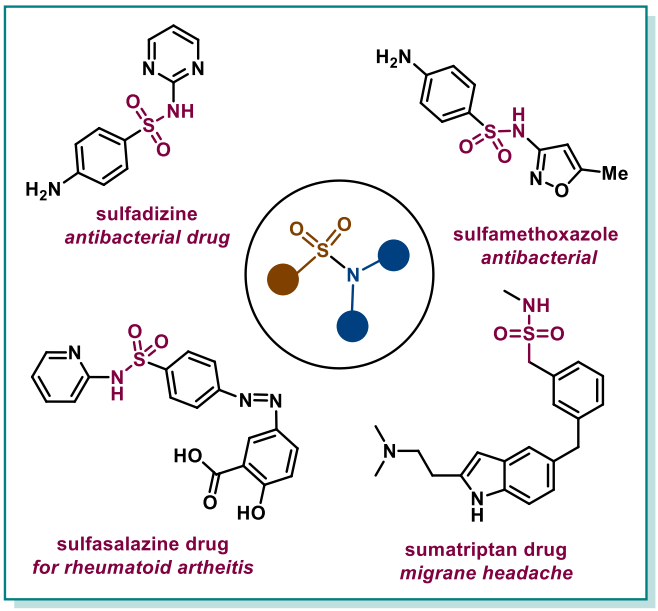

Figure 5.1 Biologically active sulfonamides

The fundamental reaction involves pairing an amine with a corresponding activated sulfonyl derivative, typically a sulfonyl chloride [4, 9-12]. Although this method is dependable, its applicability is constrained by the nucleophilicity of amines, accessibility and stability of

specific sulfonyl chlorides, and the compatibility of reaction conditions with various functional groups. Other sulfur-based substituents have also been employed for sulfonylation to access sulfonamide [13-17]. Direct multicomponent synthesis of sulfonamides by inserting a sulfur dioxide molecule between suitable carbon and nitrogen fragments through successive C−S and S−N coupling would be a more desirable but challenging alternative [18-22]. However, there remains a significant demand for more straightforward and more efficient methods for sulfonamide synthesis, as existing approaches often involve unwanted steps, generate waste, and are expensive. These concerns could be resolved by establishing an accessible and affordable process for producing sulfonamides using abundant and inexpensive reagents. Lately, there have been reports of transforming organic thiols into sulfonamides [23,24]. Nonetheless, achieving a suitable transformation necessitates an additional step, i.e., oxidation of thiol to sulfonyl chloride (Scheme 5.1).

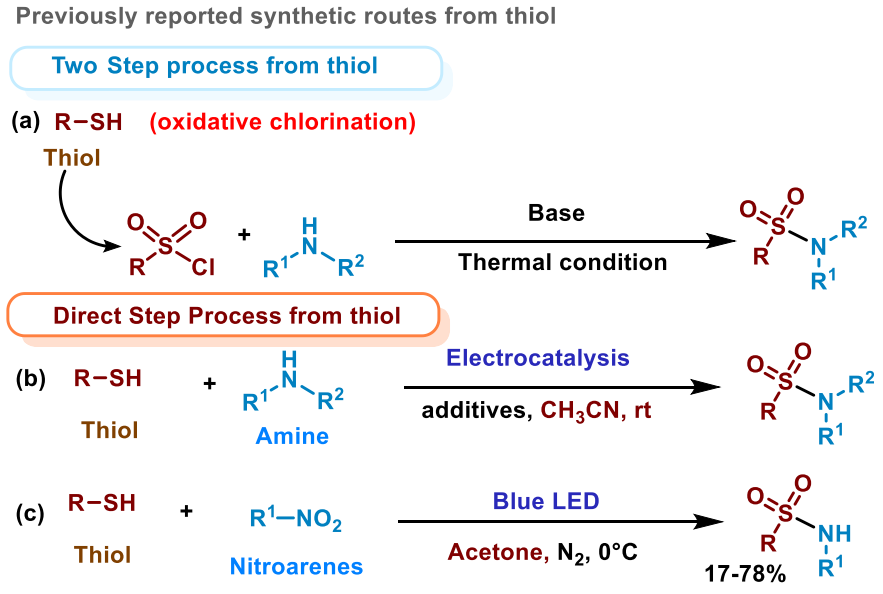

Scheme 5.1 Previous strategies for sulfonamide synthesis

Thus, establishing a direct means to obtain sulfonamides from thiols has been gaining growing interest in synthetic chemistry. An exciting and sophisticated electrochemical process for the direct synthesis of sulfonamides using amines and thiols [25] was developed by Noël (Scheme 1b). In 2022, the Chi group also directly synthesized sulfonamides by employing nitroarene for thiol amination through photo-induced oxygen atom transfer (Scheme 1c) [26].

Despite the progress made in reaching the sulfonamide framework, the potential utilization of phenylhydrazine as an amination source has not been explored [27-30]. Phenylhydrazines are an important class of inexpensive, easily accessible chemicals in organic chemistry [17, 31,32]. In recent years, with the emergence of contemporary green chemistry, metal-free photoredox catalysis, regarded as an environmentally friendly and cost-effective method, has garnered growing interest [33-39].

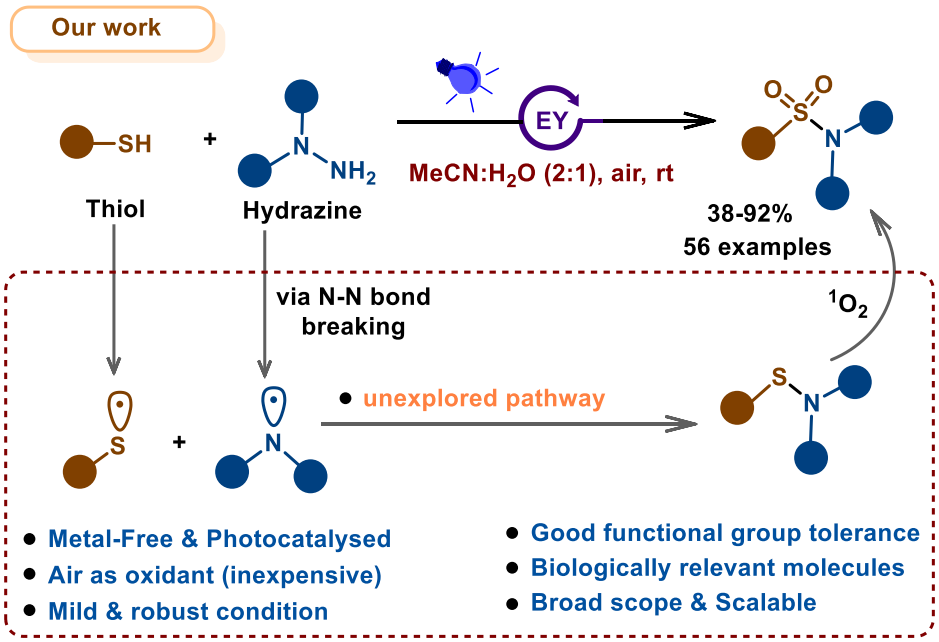

Scheme 5.2 Our strategy for sulfonamide synthesis

As our continued interest in metal-free photoredox catalysis [40-46], herein we have developed a photo-induced facile, effective, green, and metal-free approach for the synthesis of sulfonamide via oxidative sulfonylation of phenylhydrazines using thiols (Scheme 5.2).

5.2 Results and Discussion

Acknowledging the significance of sulfonamide, we preliminary explored our approach to combine benzenethiol **(1a)** as a sulfur source and phenylhydrazine **(2a)** as an amine source. We were delighted to achieve a 30% product yield at the outset of our optimization, employing benzenethiol (1 equiv.) and phenylhydrazine (1 equiv.) using eosin Y as photocatalyst in ethanol as a solvent for 14 h, under ambient air at room temperature (Table 5.1, entry 1).

Table 5.1 Optimization table for reaction conditions [(a)]

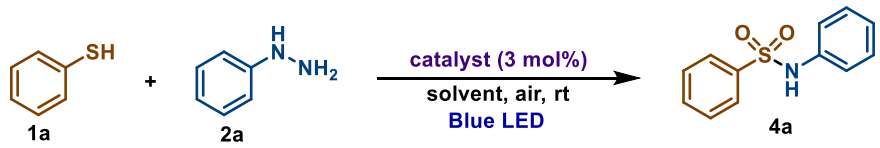

Entry	Catalyst	Solvent	Yield [(b)] (%)
1	Eosin Y	EtOH	30
2	Rose Bengal	EtOH	Trace
3	Rhodamine B	EtOH	Trace
4	Acridine Red	EtOH	Trace
5	Eosin Y	Methanol	27
6	Eosin Y	H_2O	49
7	Eosin Y	MeCN	54
8	Eosin Y	THF	28

9	Eosin Y	DMSO	29
10	Eosin Y	DMF	25
11	Eosin Y	Acetone	32
12	Eosin Y	Toluene	16
13	Eosin Y	Benzene	11
14	Eosin Y	DCM	14

[a]Reaction Condition: benzenethiol (0.25 mmol), phenylhydrazine (0.25 mmol), catalyst (3 mol %), solvent (5mL), blue LED (14h) under open air at room temperature. [b]isolated yield

Table 5.2 Different ratio of MeCN:Water screening [a]

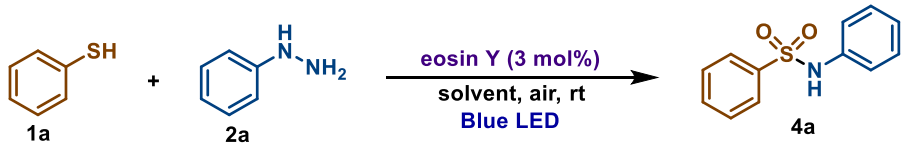

Entry	Ratio of MeCN:H_2O	Yield [b] (%)
1	MeCN:H_2O (1:1)	63
2	MeCN:H_2O (2:1)	85
3	MeCN:H_2O (1:2)	71
4	MeCN:H_2O (1:3)	76
5	MeCN:H_2O (1:4)	73
6	MeCN:H_2O (3:1)	81

[a]Reaction Condition: benzenethiol (0.25 mmol), phenylhydrazine (0.25 mmol), eosin Y (3 mol %), MeCN:H_2O (5mL), blue LED (14h) under open air at room temperature. [b]isolated yield

Replacing eosin Y with different photocatalysts diminished the desired product's yield (Table 5.1, entries 2-4). Several polar and non-polar solvents were screened in place of ethanol (Table 5.1, entries 5-14). The results showed that polar solvents produced yields between 25% and 49% and non-polar solvents between 11% and 16%. Motivated by the most significant yield in MeCN (54%) and H_2O (49%), we experimented with various MeCN to H_2O ratios (Table 5.2, entries 1-6). Optimization suggested that the amount of water significantly impacts this reaction. We concluded that the ratio of 2:1 was the optimal solvent, increasing the yield to 85%.

Table 5.3 Amount of photocatalyst and reaction time screening [(a)]

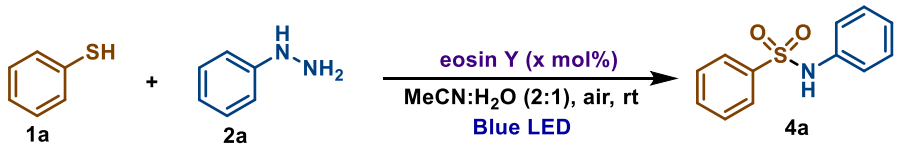

Entry	Eosin Y (mol %)	Time (h)	Yield [(b)] (%)
1	3	14	85
2	1	14	67
3	2	14	70
4	4	14	74
5	3	12	75
6	3	16	81
7	3	18	83

[(a)]Reaction Condition: benzenethiol (0.25 mmol), phenylhydrazine (0.25 mmol), eosin Y (3 mol %), MeCN:H_2O (2:1) (5 mL), blue LED under open air at room temperature. [(b)]isolated yield

There was a decrease in the yield of the product, either by increasing or decreasing the mol% of the photocatalyst (Table 5.3, entries 1-4). Extending the reaction time did not result in any noticeable increase in the product yield (Table 5.3, entries 5-7). The blue LEDs have a compelling impact on the reaction yield as the yield was decreased on using different colour LEDs (Table 5.4, entries 2-6). No results were obtained when the process was carried out without a photocatalyst, indicating the catalyst's necessity (Scheme 5.3d). These comprehensive experiments showed that the best result was obtained when eosin Y was used in 3 mol% in MeCN:H_2O (2:1, 5 mL) under blue light irradiation (14h).

Table 5.4 Screening of different color LED [(a)]

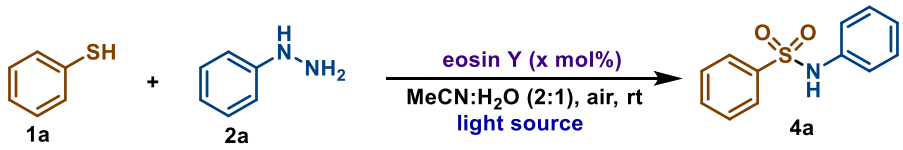

Entry	variations in the reaction conditions	Yield (%)[b]
1	in dark	nr
2	green LEDs instead of blue LEDs	54
3	purple LEDs instead of blue LEDs	62
4	White LEDs instead of blue LEDs	71
5	20W CFL instead of blue LEDs	67
6	blue LEDs	85

[(a)]Reaction Condition: benzenethiol (0.25 mmol), phenylhydrazine (0.25 mmol), eosin Y (3 mol %), MeCN:H_2O (2:1) (5mL), in visible light (14 h) under open air at room temperature. [(b)]isolated yield

Control experiments showed that light and oxygen were significant for oxidative coupling as no product was obtained in the dark or the N_2 atmosphere (Scheme 5.3e). We conducted the reaction under an external O_2 atmosphere and observed no notable variance in the product yield, indicating the involvement of atmospheric oxygen in the oxidation process (Scheme 5.3f).

Having established the optimized reaction condition in hand, we next explored the generality of the photo-induced sulfonylation of phenylhydrazines (Table 5.5). As shown in Table 5.5(a), a wide range of phenylhydrazines could be involved. Phenylhydrazines with a range of electron-donating such as methyl and acetyl **(3a, 3b)**, and electron-withdrawing such as nitro and trifluoromethyl **(3c, 3d)** substituents afforded the desired products in good to excellent yields **(72-92%)**. Substrates having Cl and Br were well tolerated with 70-71% yield **(3e, 3f)**. Additionally, we examined the steric effect on the reaction under model reaction conditions. A wide range of *ortho*-substituted **(3g-3j)** and *meta*-substituted **(3k)** arylhydrazines can function as efficient binding substances in the process, giving a good yield (60-85%) of the desired product.

Disubstituted arylhydrazines **(3l, 3m)** responded well to the reaction conditions and produced synthetically beneficial yields (58-67%). Polycyclic arylhydrazine like 2-naphthyl **(3n)** achieved the product in good yield (80%). Notably, heterocyclic substituted hydrazines were well employed, and desired products **(3o-3t)** were obtained in 38-65% yields. To further showcase the practical applicability of this method, we employed cyclopropyl **(3u)** and cyclohexyl **(3v)** substituted hydrazine to furnish the desired products in 48% and 78% yield respectively.

Table 5.5 Substrate scope for phenylhydrazines and thiols [a]

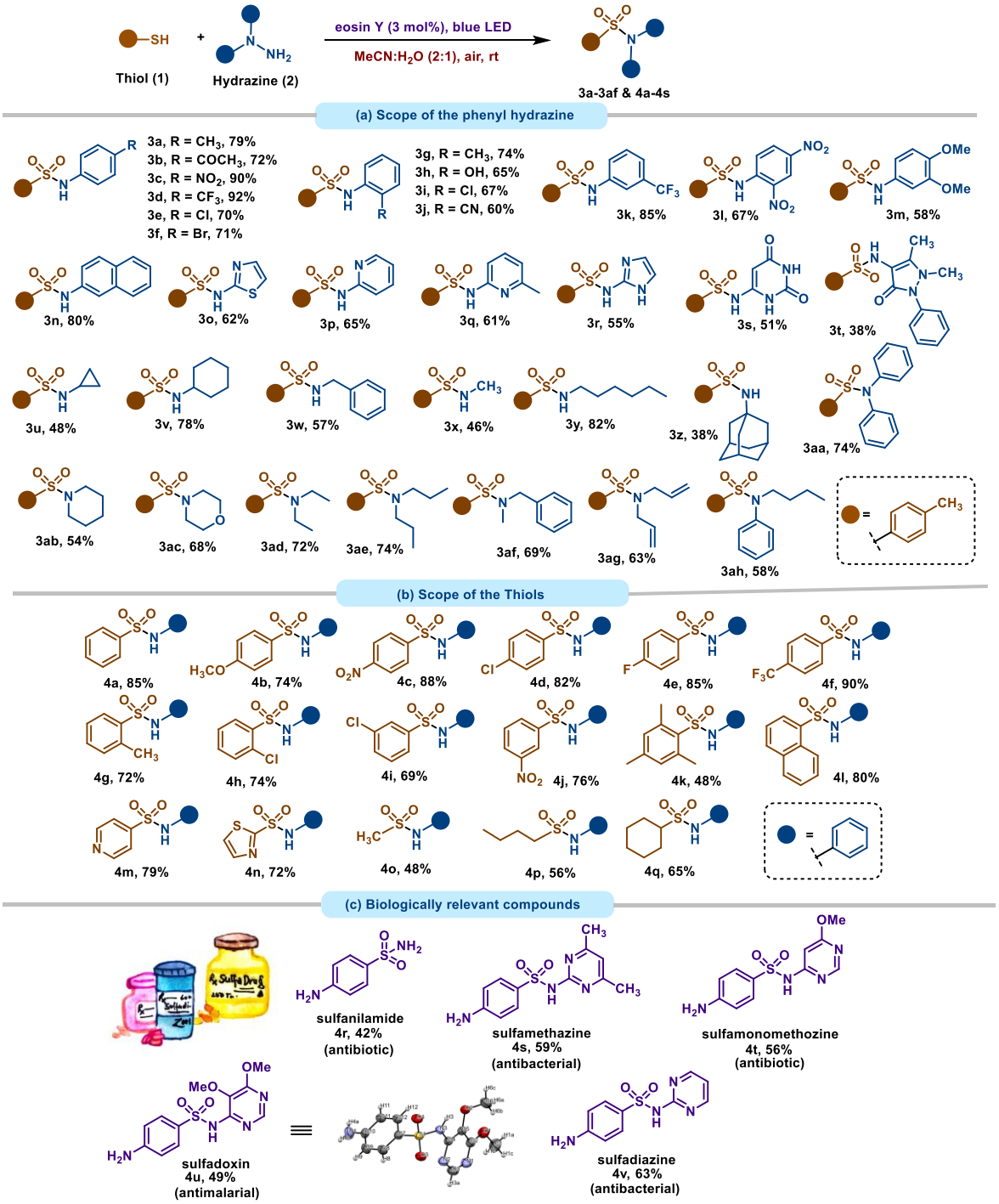

[a]Reaction Condition: benzenethiol (0.25 mmol), phenylhydrazine (0.25 mmol), eosin Y (3 mol %), MeCN:H_2O (2:1) (5mL), in visible light (14h) under open air at room temperature. [b]isolated yield

To our delight, aliphatic hydrazines like benzyl, methyl, and *n-hexyl* worked well to afford the products **(3w-3z)** in 38-82% yields. In the subsequent step, *N*-substituted hydrazines were investigated, resulting in the desired product **(3aa-3ah)** with a 54% to 74% yields.

Next, we investigated the flexibility of thiol for the sulfonylation of phenylhydrazine (Table 5.5b). Electronically neutral (-H), electron-rich (-OCH_3), and electron-deficient (-NO_2) thiols reacted smoothly, giving the desired products in 74-88% yield **(4a-4c)**. Heteroaromatic thiols having chloro, fluoro, and trifluoromethyl groups afforded the products **(4d-4f)** in 82-90% yields. There was a slight decrease in the yield when sterically hindered groups were employed. *Ortho*-substituted **(4g, 4h)**, and *meta*-substituted **(4i, 4j)** thiols exhibited the desired product in 69-76% yields.

Interestingly, trisubstituted functioned smoothly under optimal conditions (**4k,** 48%). Polycyclic thiol derivative, 2-naphthyl (**4l**) furnished the targeted product with an 80% yield. Heterocyclic thiol performed well, yielding the targeted product (**4m, 4n**) in 79% and 72% yield. Aliphatic thiol also proved effective for the coupling reaction, furnishing the target product in a 48-65% yield **(4o-4q)**. To assess the compatibility of our reaction with various functional groups (Table 5.5c), we synthesized biologically active molecules such as sulfanilamide **(4r)**, sulfamethazine **(4s)**, sulfamonomethoxine **(4t)**, sulfadoxin **(4u)**, and sulfadiazine **(4v)** in 42-63% yields. Thiols having electron-donating, electron-withdrawing, sterically hindered as well as heterocyclic thiols give good to excellent yields. Furthermore, this protocol exhibited compatibility with the gram scale, with minimal variation in the yield of product **4a** observed when the reaction was conducted on a 5.0 mmol scale (76% yield).

5.3 Control Experiments

We conducted a series of control experiments to enhance our understanding of the coupling reaction's mechanism (Scheme 5.3). We performed UV-visible spectroscopy of reactants, reaction mixture, and eosin Y (Figure 5.2). The results revealed that the reactants exhibited no absorbance in the visible region, while both the reaction mixture and eosin Y displayed absorbance in the visible region. Following that, we conducted a series of fluorescence quenching experiments, demonstrating that excited eosin Y was effectively quenched by **1a** and **2a** separately (Figure 5.3 a-b). A linear correlation between the excited state quenching of photocatalyst and concentration of **1a** and **2a** was observed, indicating a direct interaction between excited eosin Y and **1a** and **2a**, respectively (Figure 5.4). We attempted to quench the excited state of **2a** with **1a**; however, no quenching was observed, thus excluding the possibility of a direct interaction between **2a** and **1a** (Figure 5.3c). This outcome supported our hypothesis that excited eosin Y was directly reduced by **1a** and **2a**. We conducted a light ON-OFF experiment, which revealed that continuous light irradiation was necessary for product formation (Figure 5.5).

Next, we conducted the model reaction in the presence of TEMPO (a radical scavenger), a reduced yield of desired product **4a** was observed, and the analysis via high-resolution mass spectrometry (HRMS) detected the formation of a coupling adduct **5a**, **6a**, **7a**, and **8a** (Scheme 5.3a). This finding supports our point that the reaction follows a radical-driven process.

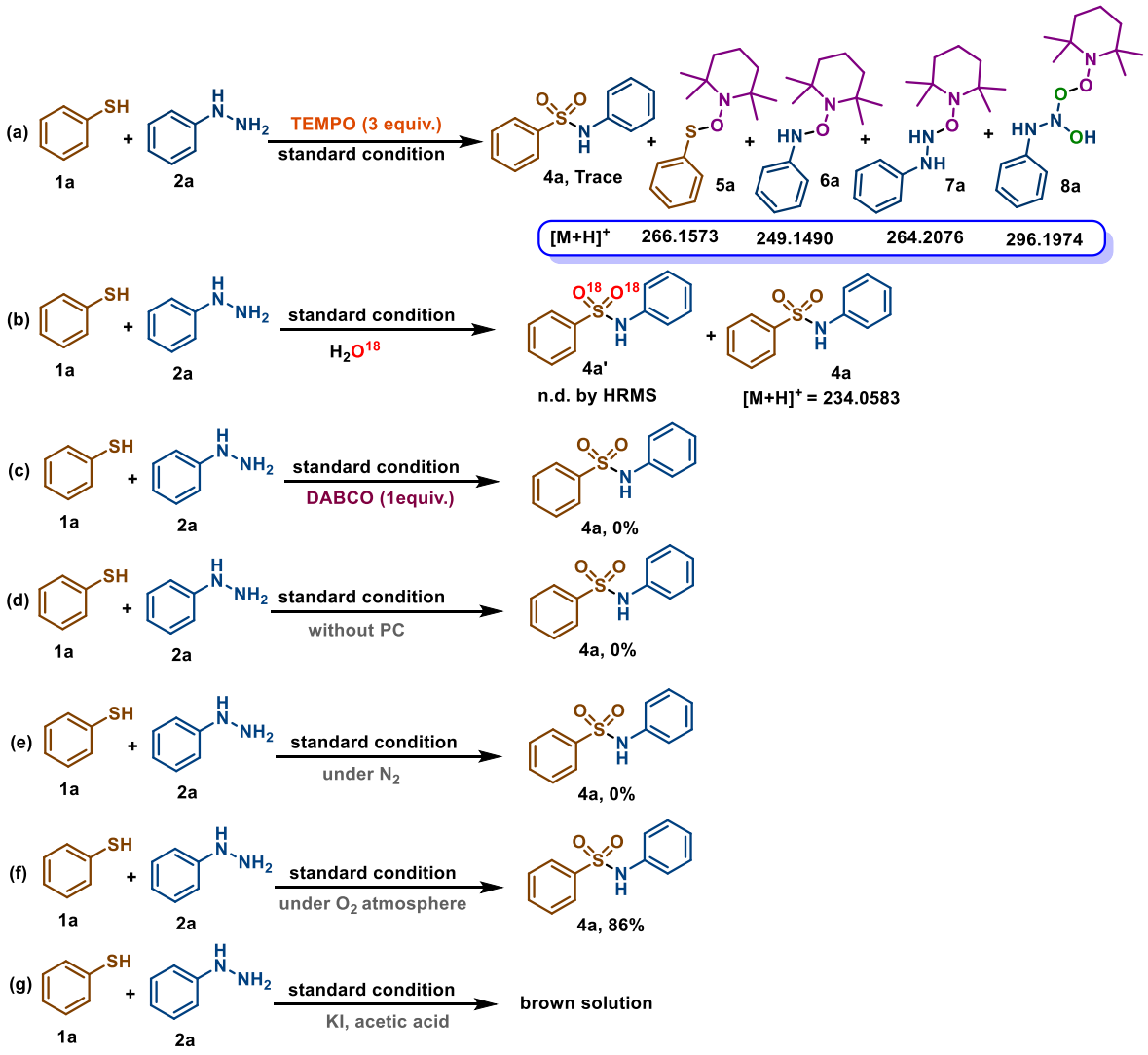

Scheme 5.3 Mechanistic Investigation

To conclusively determine the origin of the oxygen atom responsible for the oxidation, whether from air or water, an isotope-labeling experiment was conducted in the presence of H_2O^{18}. Notably, no isotope-labeled product was observed in the reaction (Scheme 5.3b). This observation unequivocally eliminates the involvement of oxygen from water molecules in the process. The addition of DABCO, employed as a singlet oxygen ($^1O_2$) physical quencher, entirely suppresses the formation of the desired product (Scheme 5.3c). This observation

strongly suggests the involvement of singlet oxygen in this transformation. On addition of acetic acid and KI in the reaction mixture, the solution turns brown which indicates the presence of H_2O_2 in the reaction mixture. Thus eliminating the reaction between formed H_2O_2 and HNO_3 (Scheme 5.3g).

5.3.1 UV-Vis absorption experiment

To prepare the sample, **1a**, **2a**, and a mixture (**1a**+**2a**+eosin Y) were dissolved in ethanol solvent, with a concentration of the reaction mixture set at 1.25×10^{-3} mol/L. The absorption spectra were measured, and the results are presented in Figure 5.2.

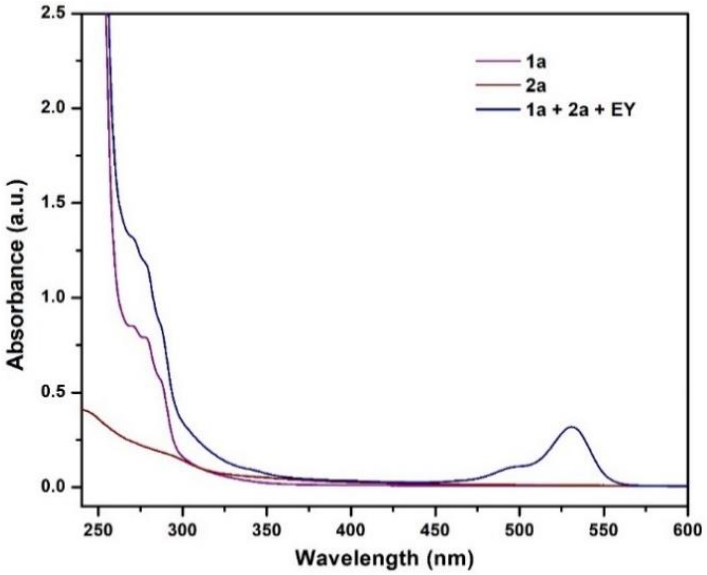

Figure 5.2 UV-Vis absorption spectra

5.3.2 Stern-Volmer Fluorescence Quenching Studies

In the fluorescence experiment, the solution of **1a** in ethanol was incrementally added to the appropriate amount of eosin Y (EY). This process was repeated five consecutive times, and emission spectra were recorded after each addition. The solutions were excited at 551 nm,

and emission was measured across the range of 0 nm to 625 nm. As depicted in Figure 5.3a, the results indicate that **1a** effectively quenches the excited state of EY and its emission. Similarly, the fluorescence quenching of eosin Y with **2a**, and **2a** with **1a** was conducted following the same procedure, as illustrated in Figure 5.3b and Figure 5.3c, respectively.

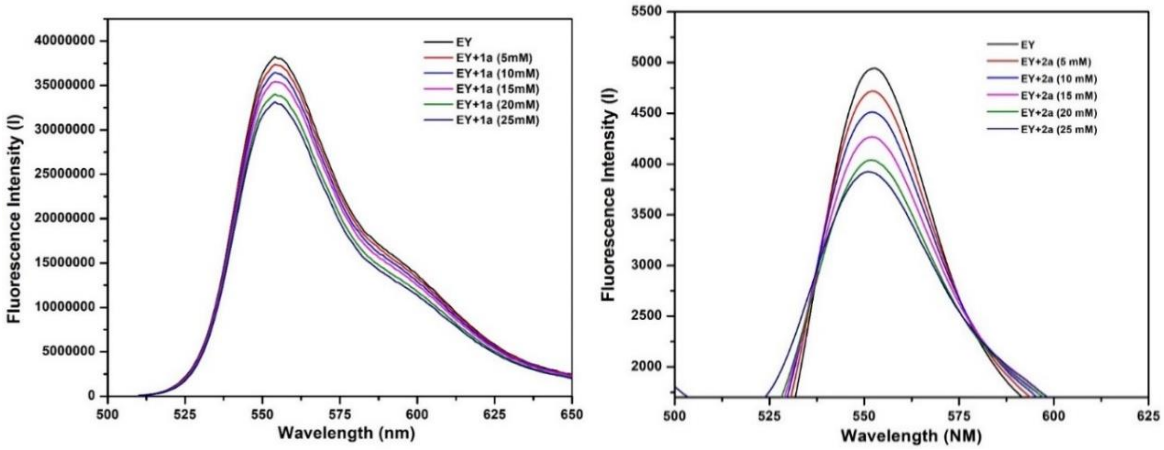

Figure 5.3a-b The fluorescence spectra of EY with different conc. of quencher **1a and 2a**

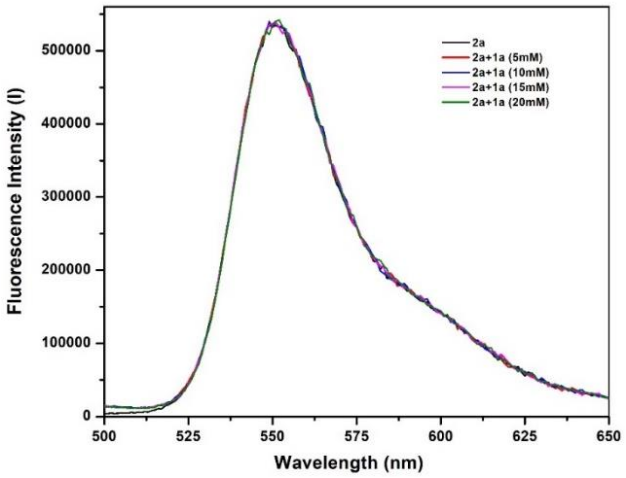

Figure 5.3c The fluorescence spectra of **2a** with different conc. of quencher **1a**

The Stern-Volmer plot (Figure 5.4) indicated a linear relationship between the quencher concentrations and the ratio I_0/I. The Stern-Volmer constant K_{SV} was calculated using equation 1.

$I_0/I = 1 + K_{SV}[Q]$ …….**Eq. 1**

Where I_0 = the intensity of fluorescence of EY, without a quencher

I = the intensity of fluorescence of EY, with a quencher

[Q] = concentration of the quencher

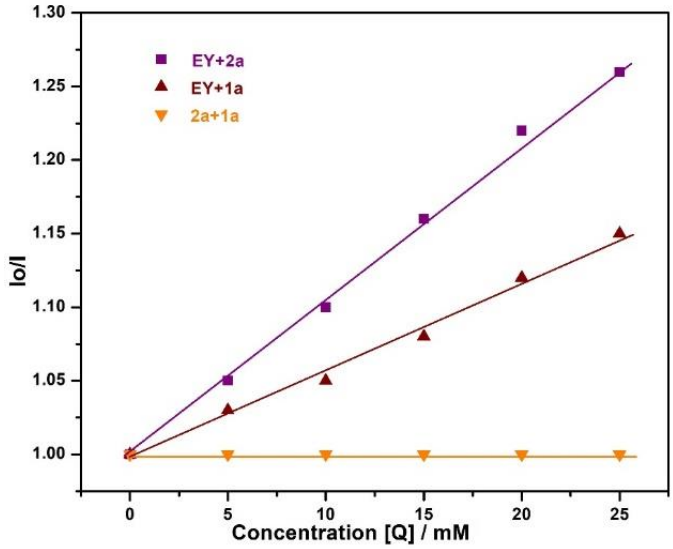

Figure 5.4 Stern-Volmer plot with different conc. of quencher

5.3.3 ON-OFF Experiments

Under the specified conditions, a reaction involving 0.25 mmol of **1a** and **2a** was conducted. The procedure involved alternating intervals of stirring the reaction mixture in the presence of visible light (blue LED) and subsequent stirring in the absence of light. At designated time points, one reaction system was halted, and the resulting mixture was later subjected to

purification through column chromatography to obtain the corresponding product **4a**. The yield of **4a** was calculated based on the weight of the product (Figure 5.5).

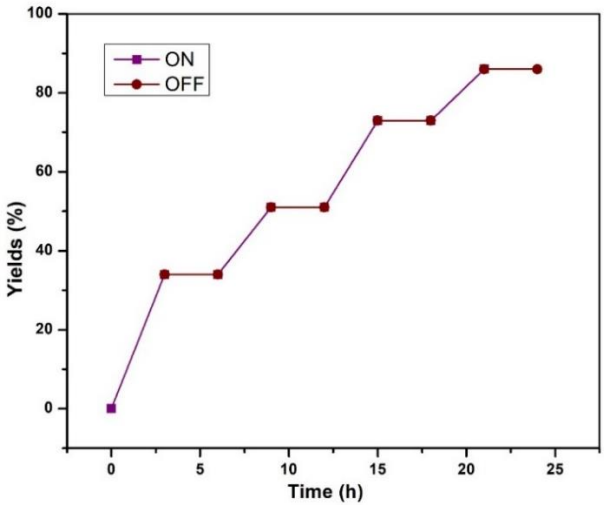

Figure 5.5 Light ON-OFF experiment

5.4 Structure determination via X-ray crystallographic analysis

The white single crystals of the compound **4u** suitable for X-ray crystallography were obtained when the saturated solution of **4u** in ethanol was prepared and the resulting solution was slowly evaporated.

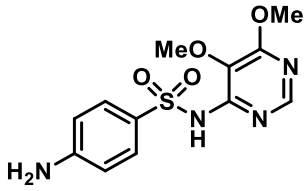

Sulfadoxin (**4u**)

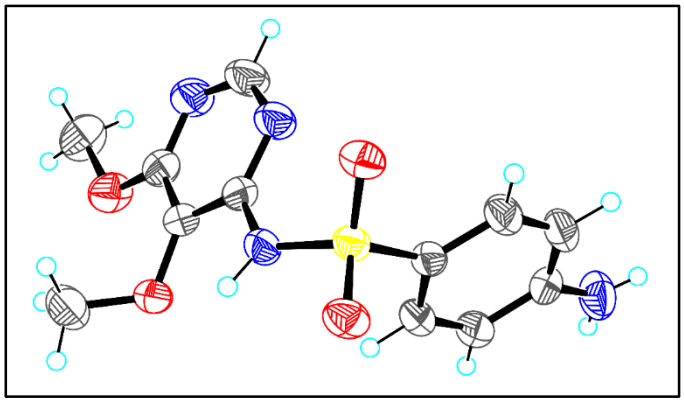

Figure 5.6 ORTEP representation crystal structure of product **4u** (ellipsoid contours of probability levels are 50%)

Table 5.6 Crystal data and structure refinement of product 4u (CCDC: 2313046)

Identification code	CHNS_auto
Empirical formula	$C_{12}H_{14}N_4O_4S$
Formula weight	310.33
Temperature/K	293
Crystal system	monoclinic
Space group	$P2_1/n$
a/Å	8.87090(10)
b/Å	8.79020(10)
c/Å	18.3310(2)
α/°	90
β/°	99.8360(10)
γ/°	90
Volume/Å^3	1408.39(3)
Z	4
ρ_{calc}g/cm^3	1.464
μ/mm^{-1}	2.262
F(000)	648.0
Crystal size/mm^3	0.25 × 0.2 × 0.2
Radiation	Cu Kα (λ = 1.54184)
2Θ range for data collection/°	9.794 to 143.906
Index ranges	$-10 \leq h \leq 10$, $-10 \leq k \leq 10$, $-22 \leq l \leq 18$
Reflections collected	15439
Independent reflections	2771 [R_{int} = 0.0364, R_{sigma} = 0.0246]
Data/restraints/parameters	2771/0/201
Goodness-of-fit on F^2	1.059
Final R indexes [I>=2σ (I)]	R_1 = 0.0359, wR_2 = 0.1010
Final R indexes [all data]	R_1 = 0.0405, wR_2 = 0.1055
Largest diff. peak/hole / e Å^{-3}	0.33/-0.37

5.5 Proposed Mechanism

Based on the control experiments and previous reports [27,47,48], we propose a plausible mechanism for thiol and phenylhydrazine coupling reaction (Scheme 5.4). Under visible

light irradiation, eosin Y undergoes photoexcitation. Phenylhydrazine reductively quenches the excited state photocatalyst EY* via single electron transfer, forming radical cation (**A**), which forms phenylhydrazine radical **B** upon deprotonation. Radical **B** captures the oxygen from the atmosphere to form radical **C**. Upon rearrangement, radical **C** forms radical E, which forms amine radical (**F**) and nitrous acid upon fragmentation. Amine radical couples with sulfenyl radical (**H**) (formed by the reductive quenching of EY*), forming intermediate **I**. Intermediate **I**, upon oxidation by singlet oxygen [49,50], forms the desired product.

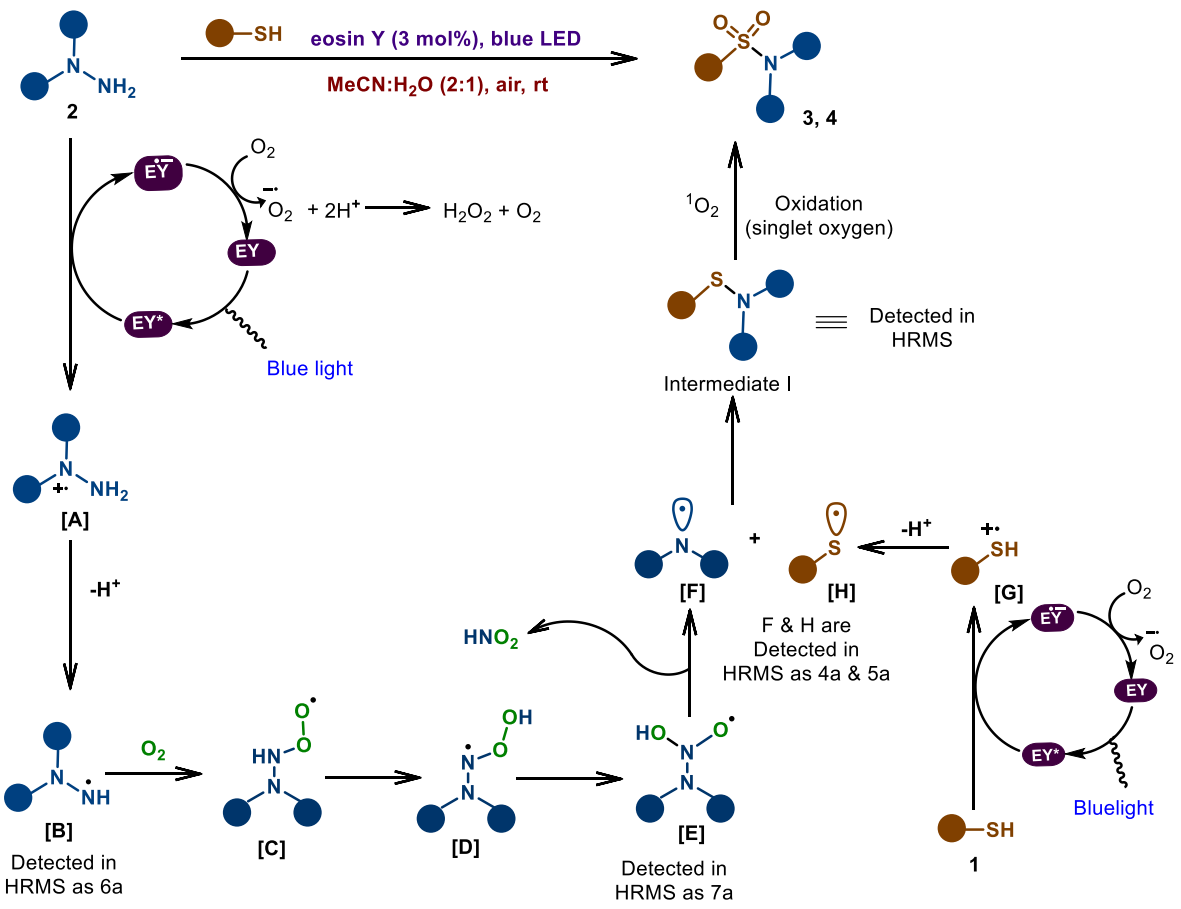

Scheme 5.4 Plausible mechanism

5.6 Conclusion

In conclusion, we have developed a practical and synthetically favourable eosin Y catalyzed method for the direct sulfonylation of hydrazines using thiols to afford sulfonamides in MeCN:H_2O (2:1, 5mL) under blue light irradiation (14h). This effective transformation is enabled by utilizing hydrazine as an amine source. This method produces sulfonamide in good to excellent yield with broad substrate scope and good functional group compatibility, including a wide range of biologically active compounds. We remain hopeful that the outcomes of this method will furnish synthetic chemists with a unique set of tools for crafting diverse and privileged scaffolds in the realm of drug discovery.

5.7 Experimental Procedures

5.7.1 General procedure for the preparation of sulfonamides

In a 25 mL round-bottom flask fitted with a magnetic stirring bar, benzenethiols **1** (0.25 mmol, 1 equiv.), phenylhydrazines **2** (0.25 mmol, 1 equiv.), eosin Y (3 mol %), and solvent (MeCN:H_2O, v/v-2:1, 5 mL) were mixed. The mixture was stirred and exposed to blue LED light strips for 14 hours in an open-air environment. The progression of the reaction was tracked using TLC. Upon completion of the reaction, the resulting mixture was extracted with ethyl acetate (15 mL × 3), and the collected organic layer was dried with anhydrous Na_2SO_4. After removing the solvent under reduced pressure, the crude product was purified through silica gel column chromatography using 10% ethyl acetate/ *n*-hexane to obtain the desired products.

5.7.2 Gram scale Synthesis of Product 4a

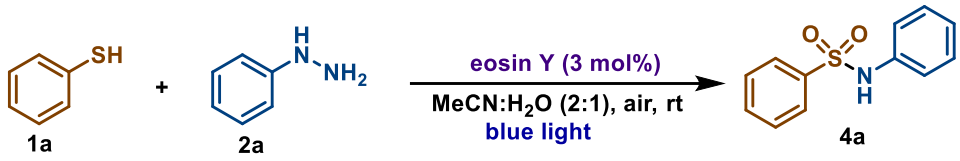

A 100 mL RB flask equipped with a magnetic stirring bar was charged with benzenethiol **1a** (0.510 mL, 5 mmol, 1.0 equiv.), phenylhydrazine **2a** (0.550 mL, 5 mmol, 1.0 equiv.), eosin Y (41.5 mg 3 mol %,), and solvent (MeCN: H_2O, v/v-2:1, 20 mL). The mixture was then stirred at room temperature and irradiated with blue LED light strips for 14 h under the open air. The progression of the reaction was tracked using TLC. Upon completion of the reaction, the resulting mixture was extracted with ethyl acetate (15 mL × 3), and the collected organic layer was dried with anhydrous Na_2SO_4. After removing the solvent under reduced pressure, the crude product was purified through silica gel column chromatography using 10% ethyl acetate/ *n*-hexane to obtain the desired products **4a** (886.5 mg, 76%).

5.8 Characterization of products

4-Methyl-N-(p-tolyl)benzenesulfonamide (3a)

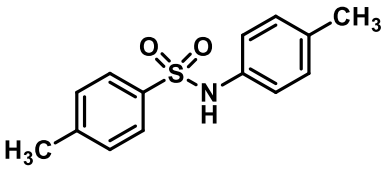

79% yield; white solid; m.p. 115-116°C; **^{1}H NMR** (500 MHz, DMSO-d_6) δ 7.54 (d, *J* = 8.3 Hz, 2H), 7.34 (d, *J* = 8.0 Hz, 2H), 7.11 (d, *J* = 3.1 Hz, 1H), 7.09 – 7.04 (m, 2H), 6.98 – 6.95 (m, 1H), 2.36 (s, 3H), 1.99 (s, 3H). **^{13}C NMR** (126 MHz, DMSO-d_6) δ 143.30, 138.47, 135.74, 134.35, 131.12, 130.00, 127.03, 126.73, 126.54, 21.43, 18.10. **HRMS** (ESI) m/z: $[M+H]^+$ calculated for $C_{14}H_{15}NO_2S$: 262.0896; found: 262.0894.

N-(4-acetylphenyl)-4-methylbenzenesulfonamide (3b)

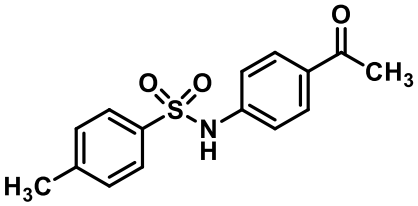

72% yield; brown solid; m.p. 200-201°C; **^{1}H NMR** (500 MHz, DMSO-d_6) δ 7.79 (d, *J* = 8.7 Hz, 2H), 7.50 (d, *J* = 8.1 Hz, 2H), 7.14 (d, *J* = 7.8 Hz, 2H), 6.86 (d, *J* = 8.6 Hz, 2H), 2.45 (s, 3H), 2.30 (s, 3H). **^{13}C NMR** (126 MHz, DMSO-d_6) δ 196.05, 145.71, 138.40, 130.80, 128.63, 125.97, 116.38, 26.60, 21.25. **HRMS** (ESI) m/z: $[M+H]^+$ calculated for $C_{15}H_{15}NO_3S$: 290.0845; found: 290.0842.

4-Methyl-N-(4-nitrophenyl)benzenesulfonamide (3c)

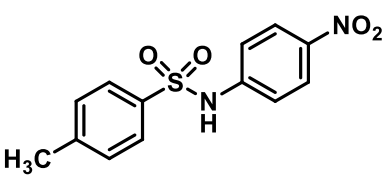

90% yield; pale gray solid; m.p. 179-180°C; **^{1}H NMR** (500 MHz, DMSO-d_6) δ 7.97 – 7.92 (m, 2H), 7.52 – 7.48 (m, 2H), 7.14 (d, *J* = 7.9 Hz, 2H), 6.62 – 6.59 (m, 2H), 2.30 (s, 3H). **^{13}C NMR** (126 MHz, DMSO-d_6) δ 156.07, 145.74, 138.39, 136.16, 128.62, 126.84, 125.97, 112.94, 21.25. **HRMS** (ESI) m/z: $[M+H]^+$ calculated for $C_{13}H_{12}N_2O_4S$: 293.0591; found: 293.0595.

4-Methyl-N-(4-(trifluoromethyl)phenyl)benzenesulfonamide (3d)

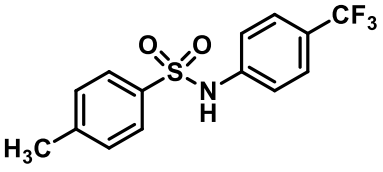

92% yield; creamy solid; m.p. 145-146°C; **^{1}H NMR** (500 MHz, DMSO-d_6) δ 10.81 (s, 1H), 7.72 (d, *J* = 8.3 Hz, 2H), 7.60 (d, *J* = 8.6 Hz, 2H), 7.37 (d, *J* = 8.0 Hz, 2H), 7.29 (d, *J* = 8.5 Hz, 2H), 2.34 (s, 3H). **^{13}C NMR** (126 MHz, DMSO-d_6) δ 144.22, 142.16, 136.82, 130.37, 127.17, 127.01, 126.98, 119.12, 21.41. **^{19}F NMR** (471 MHz, DMSO-d6) δ -60.47. **HRMS** (ESI) m/z: $[M+H]^+$ calculated for $C_{14}H_{12}F_3NO_2S$: 316.0614; found:316.0618

N-(4-chlorophenyl)-4-methylbenzenesulfonamide (3e)

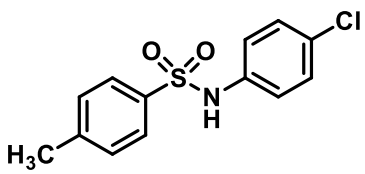

70% yield; white solid; m.p. 120-121°C; **^{1}H NMR** (500 MHz, DMSO-d_6) δ 7.63 (d, *J* = 8.0 Hz, 2H), 7.32 (d, *J* = 7.9 Hz, 2H), 7.24 (d, *J* = 8.6 Hz, 2H), 7.06 (d, *J* = 8.6 Hz, 2H), 2.32 (s, 3H). **^{13}C NMR** (126 MHz, DMSO-d_6) δ 143.31, 138.86, 137.81, 130.05, 129.38, 127.41, 127.10, 121.96, 21.39. **HRMS** (ESI) m/z: $[M+H]^+$ calculated for $C_{13}H_{12}ClNO_2S$: 282.0350; found: 282.0353

N-(4-bromophenyl)-4-methylbenzenesulfonamide (3f)

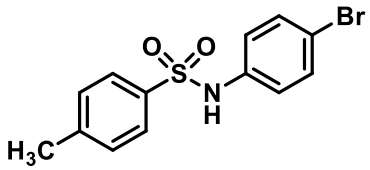

71% yield; white solid; m.p. 142-143°C; **^{1}H NMR** (500 MHz, DMSO-d_6) δ 10.88 (s, 1H), 7.94 (s, 1H), 7.87 (d, *J* = 7.6 Hz, 1H), 7.70 (d, *J* = 8.2 Hz, 2H), 7.57 – 7.50 (m, 2H), 7.38 (d, *J* = 8.1 Hz, 2H), 2.33 (s, 3H). **^{13}C NMR** (126 MHz, DMSO-d_6) δ 148.65, 144.37, 139.67, 136.50, 131.28, 130.44, 127.18, 125.68, 118.80, 113.69, 21.43. **HRMS** (ESI) m/z: $[M+H]^+$ calculated for $C_{13}H_{12}BrNO_2S$: 325.9845; found:325.9849

4-Methyl-N-(o-tolyl)benzenesulfonamide (3g)

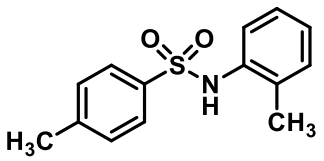

74% yield; pink solid; m.p. 105-106°C; **^{1}H NMR** (500 MHz, DMSO-d_6) δ 9.55 (s, 1H), 7.49 (d, *J* = 8.1 Hz, 2H), 7.34 – 7.32 (m, 1H), 7.30 (d, *J* = 2.2 Hz, 1H), 7.29 (d, *J* = 1.7 Hz, 1H), 7.29 – 7.27 (m, 1H), 7.12 (d, *J* = 7.8 Hz, 2H), 2.30 (d, *J* = 6.1 Hz, 6H). **^{13}C NMR** (126 MHz, DMSO-d_6) δ 146.10, 138.14, 131.79, 131.47, 128.54, 128.02, 127.63, 125.96, 123.09, 21.25, 17.29. **HRMS** (ESI) m/z: $[M+H]^+$ calculated for $C_{14}H_{15}NO_2S$: 262.0896; found:262.0894.

N-(2-hydroxyphenyl)-4-methylbenzenesulfonamide (3h)

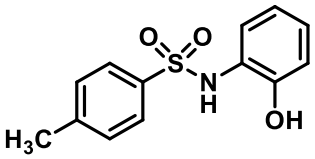

65% yield; gray solid; m.p. 139-140°C; **^{1}H NMR** (500 MHz, DMSO-d_6) δ 10.65 (s, 1H), 9.65 (s, 1H), 7.49 (d, *J* = 8.0 Hz, 2H), 7.28 – 7.22 (m, 2H), 7.12 (d, *J* = 7.8 Hz, 2H), 7.03 – 7.00 (m, 1H), 6.89 (td, *J* = 7.7, 1.2 Hz, 1H), 2.29 (s, 3H). **^{13}C NMR** (126 MHz, DMSO-d_6) δ 151.04, 146.21, 138.08, 129.70, 128.52, 125.96, 124.35, 120.00, 116.60, 21.25. **HRMS** (ESI) m/z: $[M+H]^+$ calculated for $C_{13}H_{13}NO_3S$: 264.0689; found:264.0685.

N-(2-chlorophenyl)-4-methylbenzenesulfonamide (3i)

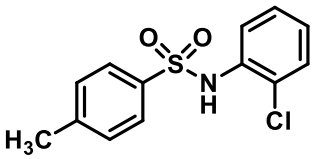

67% yield; white solid; m.p. 100-101°C; **^{1}H NMR** (500 MHz, DMSO-d_6) δ 7.50 (d, *J* = 8.1 Hz, 2H), 7.39 (dd, *J* = 8.0, 1.3 Hz, 1H), 7.25 – 7.20 (m, 1H), 7.15 – 7.12 (m, 3H), 6.96 (td, *J* = 7.9, 1.5 Hz, 1H), 6.79 (s, 1H), 2.30 (s, 3H). **^{13}C NMR** (126 MHz, DMSO-d_6) δ 145.67, 138.44, 130.10, 128.64, 128.57, 125.97, 123.14, 122.08, 120.24, 21.26. **HRMS** (ESI) m/z: $[M+H]^+$ calculated for $C_{13}H_{12}ClNO_2S$: 282.0350; found:282.0355.

N-(2-cyanophenyl)-4-methylbenzenesulfonamide (3j)

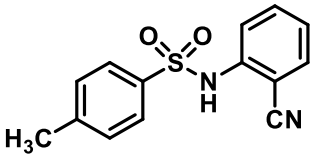

60% yield; white solid; m.p. 170-171°C; **^{1}H NMR** (500 MHz, DMSO-d_6) δ 7.51 (d, J = 8.1 Hz, 2H), 7.38 (dd, J = 7.8, 1.4 Hz, 1H), 7.30 (ddd, J = 8.6, 7.2, 1.6 Hz, 1H), 7.14 (dd, J = 8.3, 0.5 Hz, 2H), 6.82 – 6.78 (m, 1H), 6.63 – 6.58 (m, 1H), 2.30 (s, 3H). **^{13}C NMR** (126 MHz, DMSO-d_6) δ 151.73, 145.56, 138.50, 134.43, 132.91, 128.66, 125.98, 118.54, 116.62, 115.85, 94.16, 21.26. **HRMS** (ESI) m/z: $[M+H]^+$ calculated for $C_{14}H_{12}N_2O_2S$: 273.0692; found:273.0695.

4-Methyl-N-(3-(trifluoromethyl)phenyl)benzenesulfonamide (3k)

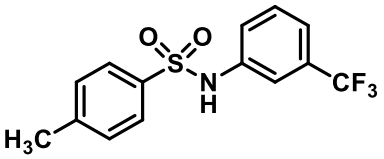

85% yield; white solid; m.p. 115-116°C; **^{1}H NMR** (500 MHz, DMSO-d_6) δ 7.57 (t, *J* = 7.9 Hz, 1H), 7.50 (d, *J* = 8.1 Hz, 2H), 7.46 (s, 1H), 7.42 (s, 1H), 7.38 (d, *J* = 8.0 Hz, 1H), 7.14 (d, *J* = 7.9 Hz, 2H), 2.30 (s, 3H). **^{13}C NMR** (126 MHz, DMSO-d_6) δ 145.56, 138.50, 131.20, 130.63, 130.38, 128.64, 125.95, 120.62, 116.72, 21.24. **^{19}F NMR** (471 MHz, DMSO-d6) δ -61.43. **HRMS** (ESI) m/z: $[M+H]^+$ calculated for $C_{14}H_{12}F_3NO_2S$: 316.0614; found:316.0619.

N-(2,4-dinitrophenyl)-4-methylbenzenesulfonamide (3l)

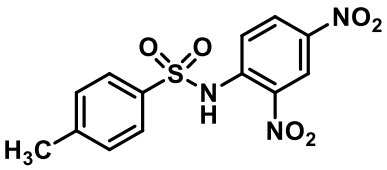

67% yield; light brown; m.p. 121-122°C; **^{1}H NMR** (500 MHz, DMSO-d_6) δ 8.80 (d, *J* = 2.7 Hz, 2H), 8.38 (s, 2H), 8.18 (d, *J* = 2.7 Hz, 1H), 8.16 (d, *J* = 2.7 Hz, 1H), 7.12 (d, *J* = 9.4 Hz, 2H), 2.09 (s, 3H). **^{13}C NMR** (126 MHz, DMSO-d_6) δ 150.29, 135.60, 129.78, 129.16, 123.86, 120.25. **HRMS** (ESI) m/z: $[M+H]^+$ calculated for $C_{13}H_{11}N_3O_6S$: 338.0441; found:338.0445.

N-(3,4-dimethoxyphenyl)-4-methylbenzenesulfonamide (3m)

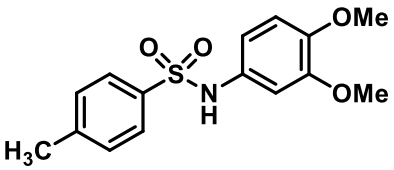

58% yield; black solid; m.p. 120-121°C; **^{1}H NMR** (500 MHz, DMSO-d_6) δ 9.86 (s, 1H), 7.60 (d, *J* = 8.3 Hz, 2H), 7.33 (d, *J* = 8.0 Hz, 2H), 6.78 (d, *J* = 8.7 Hz, 1H), 6.68 (d, *J* = 2.4 Hz, 1H), 6.54 (dd, *J* = 8.6, 2.5 Hz, 1H), 3.65 (s, 3H), 3.63 (s, 3H), 2.33 (s, 3H). **^{13}C NMR** (126 MHz, DMSO-d_6) δ 149.15, 146.44, 143.52, 137.03, 131.08, 130.01, 127.28,

113.80, 112.44, 106.76, 56.00, 55.80, 21.40. **HRMS** (ESI) m/z: $[M+H]^+$calculated for $C_{15}H_{17}NO_4S$: 308.0951; found:308.0955.

4-Methyl-N-(naphthalen-2-yl)benzenesulfonamide (3n)

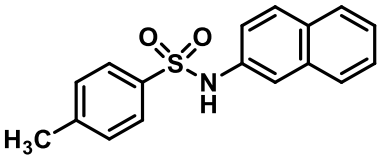

80% yield; brownish gray solid; m.p. 110-111°C; **^{1}H NMR** (500 MHz, DMSO-d_6) δ 8.05 (d, *J* = 8.8 Hz, 1H), 7.99 (d, *J* = 9.4 Hz, 2H), 7.83 (d, *J* = 2.0 Hz, 1H), 7.59 (tt, *J* = 14.6, 3.4 Hz, 2H), 7.50 – 7.48 (m, 2H), 7.45 (dd, *J* = 8.7, 2.2 Hz, 1H), 7.12 (d, *J* = 7.8 Hz, 3H), 2.29 (s, 3H). **^{13}C NMR** (126 MHz, DMSO-d_6) δ 146.03, 138.17, 133.29, 132.07, 130.34, 128.54, 128.32, 128.03, 127.76, 126.98, 125.95, 121.58, 21.24. **HRMS** (ESI) m/z: $[M+H]^+$ calculated for $C_{17}H_{15}NO_2S$: 298.0896; found:298.0899.

4-Methyl-N-(thiazol-2-yl)benzenesulfonamide (3o)

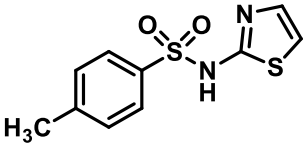

62% yield; yellow solid; m.p. 204-205°C; **^{1}H NMR** (500 MHz, DMSO-d_6) δ 12.68 (s, 1H), 7.69 (d, *J* = 8.2 Hz, 2H), 7.33 (d, *J* = 8.0 Hz, 2H), 7.24 (d, *J* = 4.6 Hz, 1H), 6.82 (d, *J* = 4.6 Hz, 1H), 2.35 (s, 3H). **^{13}C NMR** (126 MHz, DMSO-d_6) δ 169.27, 142.61, 140.01, 129.79, 126.29, 124.89, 108.59, 21.40. **HRMS** (ESI) m/z: $[M+H]^+$ calculated for $C_{10}H_{10}N_2O_2S_2$: 255.0256; found:255.0254.

4-Methyl-N-(pyridin-2-yl)benzenesulfonamide (3p)

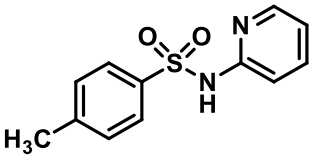

65% yield; light yellow solid; m.p. 215-216°C; **^{1}H NM**R (500 MHz, DMSO-d_6) 8.01 (d, *J* = 4.6 Hz, 1H), 7.76 (d, *J* = 8.3 Hz,

2H), 7.71 (t, *J* = 7.9 Hz, 1H), 7.34 (d, *J* = 8.0 Hz, 2H), 7.14 (d, *J* = 8.7 Hz, 1H), 6.87 (t, *J* = 6.2 Hz, 1H), 2.34 (s, 3H). **^{13}C NMR** (126 MHz, DMSO-d_6) δ 142.95, 142.17, 140.68, 129.86, 128.54, 127.08, 125.96, 114.02, 110.48, 21.40. **HRMS** (ESI) m/z: $[M+H]^+$ calculated for $C_{12}H_{12}N_2O_2S$: 249.0692; found:249.0695.

4-Methyl-N-(6-methylpyridin-2-yl)benzenesulfonamide (3q)

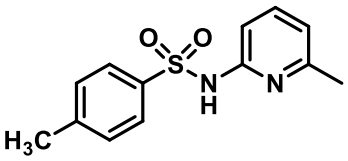

61% yield; light yellow solid; m.p. 114-115°C; **^{1}H NMR** (500 MHz, DMSO-d_6) δ 7.74 (d, *J* = 8.1 Hz, 2H), 7.60 (dd, *J* = 8.4, 7.6 Hz, 1H), 7.32 (d, *J* = 8.0 Hz, 2H), 6.99 (d, *J* = 8.4 Hz, 1H), 6.66 (d, *J* = 6.9 Hz, 1H), 2.34 (s, 3H), 2.30 (s, 3H). **^{13}C NMR** (126 MHz, DMSO-d_6) δ 157.60, 153.64, 141.92, 140.09, 137.64, 131.30, 129.70, 126.99, 118.95, 24.16, 21.37. **HRMS** (ESI) m/z: $[M+H]^+$ calculated for $C_{13}H_{14}N_2O_2S$: 263.0849; found:263.0845.

N-(1H-imidazol-2-yl)-4-methylbenzenesulfonamide (3r)

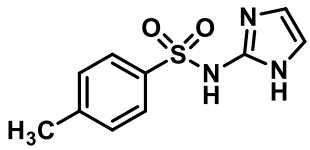

55% yield; brown solid; m.p. 138-139°C; **^{1}H NMR** (500 MHz, DMSO-d_6) δ 12.71 (s, 1H), 7.68 (d, *J* = 8.2 Hz, 2H), 7.34 (d, *J* = 7.9 Hz, 2H), 7.23 (d, *J* = 4.6 Hz, 1H), 6.81 (d, *J* = 4.6 Hz, 1H), 2.35 (s, 3H). **^{13}C NMR** (126 MHz, DMSO-d_6) δ 169.28, 142.66, 139.96, 129.81, 126.29, 124.87, 108.62, 21.39. **HRMS** (ESI) m/z: $[M+H]^+$ calculated for $C_{10}H_{11}N_3O_2S$: 238.0645; found:238.0648.

N-(2,6-dioxo-1,2,3,6-tetrahydropyrimidin-4-yl)benzenesulfonamide (3s)

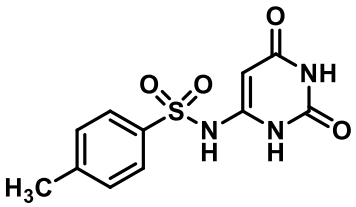

51% yield; light yellow solid; m.p. 280-281°C; **^{1}H NMR** (500 MHz, DMSO-d_6) δ 11.23 (s, 6H), 8.95 (d, *J* = 5.4 Hz, 4H), 8.65 (t, *J* = 7.7 Hz, 2H), 8.14 – 8.09 (m, 4H), 4.96 (s, 2H), 2.08 (s, 1H). **^{13}C NMR** (126 MHz, DMSO-d_6) δ 165.15, 158.15, 149.99, 147.03, 142.08, 127.86, 73.44. **HRMS** (ESI) m/z: $[M+H]^+$ calculated for $C_{11}H_{11}N_3O_4S$: 282.0543; found:282.0547.

N-(1,5-dimethyl-3-oxo-2-phenyl-2,3-dihydro-1H-pyrazol-4-yl)-4-methylbenzenesulfonamide (3t)

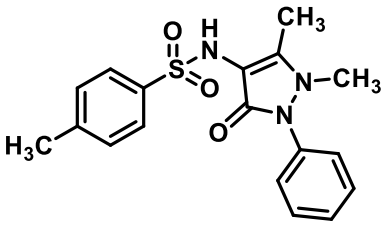

38% yield; brick red solid;. m.p. 220-221°C; **^{1}H NMR** (500 MHz, DMSO-d_6) δ 9.17 (s, 1H), 7.71 (d, *J* = 8.3 Hz, 2H), 7.47 (dd, *J* = 8.2, 7.6 Hz, 2H), 7.32 (dd, *J* = 11.5, 5.5 Hz, 3H), 7.25 (dd, *J* = 8.5, 1.1 Hz, 2H), 3.04 (s, 3H), 2.36 (s, 3H), 2.06 (s, 3H). **^{13}C NMR** (126 MHz, DMSO-d_6) δ 162.47, 155.44, 143.07, 138.80, 135.38, 129.71, 129.54, 127.35, 126.97, 124.38, 105.64, 36.03, 21.47, 10.97. **HRMS** (ESI) m/z: $[M+H]^+$ calculated for $C_{18}H_{19}N_3O_3S$: 358.1220; found:358.1223.

N-cyclopropyl-4-methylbenzenesulfonamide (3u)

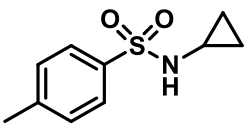

48% yield; light brown solid; m.p. 71-72°C; **^{1}H NMR** (500 MHz, DMSO-d_6) δ 7.83 (s, 1H), 7.70 (d, *J* = 8.2 Hz, 2H), 7.42 (d, *J* = 8.4 Hz, 2H), 2.40 (s, 3H), 2.06 (dt, *J* = 9.7, 3.3 Hz, 1H), 0.46 (td, *J* = 7.0, 4.7 Hz, 2H), 0.38 – 0.33 (m, 2H). **^{13}C NMR** (126 MHz, DMSO-d_6) δ 143.19, 137.88, 130.05, 127.28, 24.54, 21.45, 5.54. **HRMS** (ESI) m/z: $[M+H]^+$ calculated for $C_{10}H_{13}NO_2S$: 212.0740; found:212.0743.

N-cyclohexyl-4-methylbenzenesulfonamide (3v)

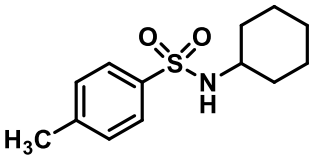

78% yield; white solid; m.p. 81-82°C; **^{1}H NMR** (500 MHz, DMSO-d_6) δ 7.69 (d, *J* = 8.2 Hz, 2H), 7.55 (d, *J* = 7.3 Hz, 1H), 7.38 (d, *J* = 7.9 Hz, 2H), 2.92 – 2.86 (m, 1H), 2.38 (s, 3H), 1.60 – 1.52 (m, 4H), 1.43 (d, *J* = 11.9 Hz, 1H), 1.13 – 1.02 (m, 5H). **^{13}C NMR** (126 MHz, DMSO-d_6) δ 142.72, 139.87, 130.00, 126.73, 52.47, 33.66, 25.31, 24.82, 21.41. **HRMS** (ESI) m/z: $[M+H]^+$ calculated for $C_{13}H_{19}NO_2S$: 254.1209; found:254.1207.

N-benzyl-4-methylbenzenesulfonamide (3w)

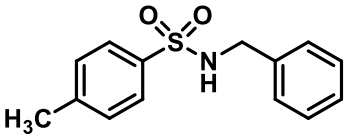

57% yield; cream white solid; m.p. 112-113°C; **^{1}H NMR** (500 MHz, DMSO-d_6) δ 8.16 (s, 1H), 7.51 – 7.48 (m, 2H), 7.48 – 7.44 (m, 2H), 7.43 (t, *J* = 3.2 Hz, 1H), 7.42 – 7.37 (m, 1H), 7.13 (d, *J* = 7.8 Hz, 2H), 4.04 (q, *J* = 5.9 Hz, 2H), 2.30 (s, 3H). **^{13}C NMR** (126 MHz, DMSO-d_6) δ 145.96, 138.24, 134.42, 129.32, 129.11, 128.98, 128.58, 125.97, 42.82, 21.25. **HRMS** (ESI) m/z: $[M+H]^+$ calculated for $C_{14}H_{15}NO_2S$: 262.0896; found:262.0894.

N,4-dimethylbenzenesulfonamide (3x)

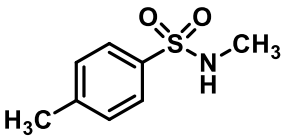

46% yield; dark brown solid; m.p. 99-100°C; **^{1}H NMR** (500 MHz, DMSO-d_6) δ 9.54 (s, 1H), 7.14 (d, *J* = 8.3 Hz, 2H), 7.12 – 7.09 (m, 2H), 2.92 (s, 3H), 2.26 (s, 3H). **^{13}C NMR** (126 MHz, DMSO-d_6) δ 136.16, 133.73, 130.17, 120.95, 39.35, 20.80. **HRMS** (ESI) m/z: $[M+H]^+$ calculated for $C_8H_{11}NO_2S$: 186.0583; found:186.0585.

N-hexyl-4-methylbenzenesulfonamide (3y)

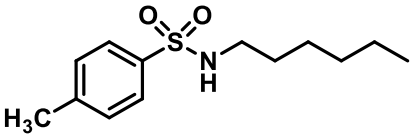

82% yield; white solid; m.p. 59-60°C; **^{1}H NMR** (500 MHz, DMSO-d_6) δ 7.68 – 7.65 (m, 2H), 7.46 (t, *J* = 5.8 Hz, 1H), 7.39 (d, *J* = 7.9 Hz, 2H), 2.69 (dd, *J* = 13.0, 7.0 Hz, 2H), 2.38 (s, 3H), 1.36 – 1.30 (m, 2H), 1.23 – 1.13 (m, 6H), 0.82 (t, *J* = 7.1 Hz, 3H). **^{13}C NMR** (126 MHz, DMSO-d_6) δ 142.93, 138.23, 130.04, 126.96, 42.96, 31.20, 29.34, 26.14, 22.41, 21.40, 14.30. **HRMS** (ESI) m/z: $[M+H]^+$ calculated for $C_{13}H_{21}NO_2S$: 256.1366; found:256.1368.

N-((3s,5s,7s)-adamantan-1-yl)-4-methylbenzenesulfonamide (3z)

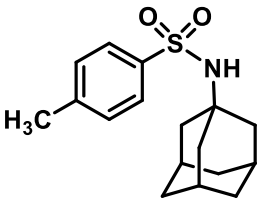

38% yield; white solid; m.p. 159-160°C; **^{1}H NMR** (500 MHz, DMSO-d_6) δ 7.72 (d, *J* = 8.3 Hz, 2H), 7.45 (s, 1H), 7.36 (d, *J* = 8.0 Hz, 2H), 2.38 (s, 3H), 1.91 (s, 3H), 1.67 (d, *J* = 2.5 Hz, 6H), 1.53 (d, *J* = 12.2 Hz, 3H), 1.46 (d, *J* = 11.4 Hz, 3H). **^{13}C NMR** (126 MHz, DMSO-d_6) δ 142.7, 142.3, 129.9, 126.5, 54.1, 42.9, 36.0, 29.2, 21.4. **HRMS** (ESI) m/z: $[M+H]^+$ calculated for $C_{17}H_{24}NO_2S$: 306.1522; found:306.1525.

4-Methyl-N,N-diphenylbenzenesulfonamide (3aa)

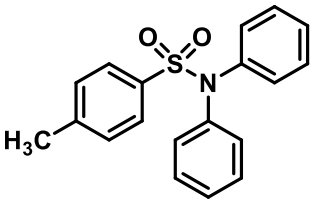

74% yield; white solid; m.p. 128-129°C; **^{1}H NMR** (500 MHz, DMSO-d_6) δ 7.63-7.67 (m, 3H), 7.55 (t, *J* = 7.6 Hz, 2H), 7.12-7.18 (m, 2H), 7.08-7.10 (m, 3H), 6.98 – 6.95 (m, 1H), 6.81 – 6.72 (m, 3H), 1.97 (s, 3H). **^{13}C NMR** (126 MHz, DMSO-d_6) δ 157.77, 141.03, 135.22, 134.63, 133.17, 131.19, 129.84, 129.63, 126.98, 126.94, 126.78, 119.28, 115.69, 17.99. **HRMS** (ESI) m/z: [M+H] + calculated for $C_{14}H_{13}NO_3S$ 323.0980; found: 323.0981

1-Tosylpiperidine (3ab)

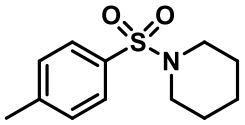

54% yield; white solid; m.p. 97-98°C; **^{1}H NMR** (500 MHz, DMSO-d_6) δ 7.61 (d, *J* = 8.3 Hz, 2H), 7.45 (d, *J* = 7.9 Hz, 2H), 2.88 – 2.82 (m, 4H), 2.41 (s, 3H), 1.53 (dt, *J* = 11.3, 5.8 Hz, 4H), 1.38 – 1.31 (m, 2H). **^{13}C NMR** (126 MHz, DMSO-d_6) δ 143.87, 132.96, 130.30, 130.22, 128.00, 127.87, 47.05, 25.12, 21.52, 21.42. **HRMS** (ESI) m/z: $[M+H]^+$ calculated for $C_{12}H_{18}NO_2S$: 240.1058; found:240.1060.

4-Tosylmorpholine (3ac)

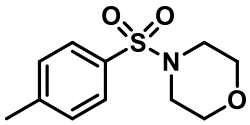

68% yield; white solid; m.p. 146-147°C; **^{1}H NMR** (500 MHz, DMSO-d_6) δ 7.63 (d, *J* = 8.3 Hz, 2H), 7.50 – 7.47 (m, 2H), 3.64 – 3.60 (m, 4H), 2.85 – 2.80 (m, 4H), 2.43 (s, 3H). **^{13}C NMR** (126 MHz, DMSO-d_6) δ 144.39, 131.83, 130.43, 128.24, 65.72, 46.36, 21.46. **HRMS** (ESI) m/z: $[M+H]^+$ calculated for $C_{11}H_{16}NO_3S$: 242.0851; found:242.0848.

N,N-diethyl-4-methylbenzenesulfonamide (3ad)

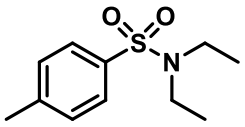

72% yield; light brown liquid; **^{1}H NMR** (500 MHz, DMSO-d_6) δ 7.67 (d, *J* = 8.3 Hz, 2H), 7.40 (d, *J* = 8.0 Hz, 2H), 3.13 (q, *J* = 7.1 Hz, 4H), 2.39 (s, 3H), 1.03 (t, *J* = 7.1 Hz, 6H). **^{13}C NMR** (126 MHz, DMSO-d_6) δ 143.38, 137.31, 130.25, 127.28, 42.24, 21.36, 14.59. **HRMS** (ESI) m/z: $[M+H]^+$ calculated for $C_{11}H_{18}NO_2S$: 228.1058; found:228.1056.

4-Methyl-N, N-dipropylbenzenesulfonamide (3ae)

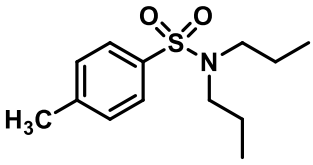

74% yield; light yellow liquid; **^{1}H NMR** (500 MHz, DMSO-d_6) δ 7.67 (d, *J* = 8.3 Hz, 2H), 7.41 (d, *J* = 7.9 Hz, 2H), 3.02 – 2.96 (m, 4H), 2.39 (s, 3H), 1.50 – 1.41 (m, 4H), 0.81 (t, *J* = 7.4 Hz, 6H). **^{13}C NMR** (126 MHz, DMSO-d_6) δ 143.36, 137.04, 130.25, 127.26, 50.15, 22.11, 21.41, 11.47. **HRMS** (ESI) m/z: $[M+H]^+$ calculated for $C_{13}H_{21}NO_2S$: 256.1366; found:256.1369.

N-benzyl-N,4-dimethylbenzenesulfonamide (3af)

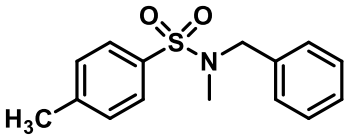

69% yield; yellow solid; m.p. 96-97^{o}C; **^{1}H NMR** (500 MHz, DMSO-d_6) δ 7.74 (d, *J* = 8.3 Hz, 2H), 7.48 (d, *J* = 7.9 Hz, 2H), 7.39 – 7.35 (m, 2H), 7.32 (dd, *J* = 6.7, 4.2 Hz, 3H), 4.10 (s, 2H), 2.51 (s, 3H), 2.43 (s, 3H). **^{13}C NMR** (126 MHz, DMSO-d_6) δ 143.91, 136.55, 134.45, 130.42, 129.04, 128.63, 128.16, 127.73, 53.80, 34.90, 21.48. **HRMS** (ESI) m/z: $[M+H]^+$ calculated for $C_{15}H_{17}NO_2S$: 276.1053; found:276.1055.

N,N-diallyl-4-methylbenzenesulfonamide (3ag)

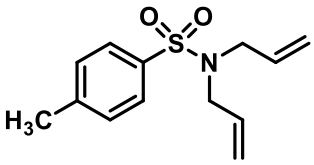

63% yield; yellow liquid; **^{1}H NMR** (500 MHz, DMSO-d_6) δ 7.71 (d, *J* = 8.3 Hz, 2H), 7.42 (d, *J* = 8.0 Hz, 2H), 5.60 (ddt, *J* = 16.4, 10.2, 6.2 Hz, 2H), 5.20 – 5.10 (m, 4H), 3.73 (d, *J* = 6.2 Hz, 4H), 2.40 (s, 3H). **^{13}C NMR** (126 MHz, DMSO-d_6) δ 143.69, 137.19, 133.34, 130.34, 127.43, 119.22, 49.81, 21.44. **HRMS** (ESI) m/z: $[M+H]^+$ calculated for $C_{13}H_{17}NO_2S$: 252.1053; found:252.1056.

N-butyl-4-methyl-N-phenylbenzenesulfonamide (3ah)

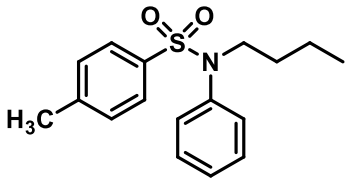

58% yield; yellow liquid; **^{1}H NMR** (500 MHz, DMSO-d_6) δ 8.95 (d, *J* = 5.2 Hz, 2H), 8.65 – 8.59 (m, 1H), 8.09 (dd, *J* = 7.7, 6.6 Hz, 2H), 7.67 (d, *J* = 8.2 Hz, 2H), 7.38 (d, *J* = 7.9 Hz, 2H), 2.68 (dd, *J* = 12.3, 6.8 Hz, 2H), 2.37 (s, 3H), 1.36 – 1.29 (m, 2H), 1.21 (dd, *J* = 15.1, 7.4 Hz, 2H), 0.77 (t, *J* = 7.3 Hz, 3H). **^{13}C NMR** (126 MHz, DMSO-d_6) δ 146.6, 142.9, 142.3, 138.1, 130.0, 127.8, 127.7, 127.0, 126.9, 42.6, 31.5, 21.4, 21.4, 19.7, 13.9. **HRMS** (ESI) m/z: $[M+H]^+$ calculated for $C_{17}H_{21}NO_2S$: 304.1366; found:304.1368.

N-phenylbenzenesulfonamide (4a)

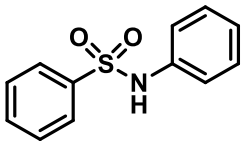

85% yield; white solid; m.p. 106-107^{o}C; **^{1}H NMR** (500 MHz, DMSO-d_6) δ 10.29 (s, 1H), 7.77 – 7.74 (m, 2H), 7.62 – 7.59 (m, 1H), 7.56 – 7.52 (m, 2H), 7.22 (dd, *J* = 8.5, 7.4 Hz, 2H), 7.09 (dd, *J* = 8.6, 1.1 Hz, 2H), 7.03 (dd, *J* = 11.6, 4.2 Hz, 1H). **^{13}C NMR** (126 MHz, DMSO-d_6) δ 139.96, 138.11, 133.35, 129.71, 129.62, 127.10, 124.58, 120.54. **HRMS** (ESI) m/z: $[M+H]^+$ calculated for $C_{12}H_{11}NO_2S$: 234.0583; found:234.0586.

4-Methoxy-N-phenylbenzenesulfonamide (4b)

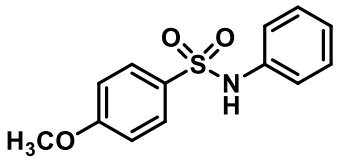

74% yield; white solid; m.p. 104-105^{o}C; **^{1}H NMR** (500 MHz, DMSO-d_6) δ 9.91 (s, 1H), 7.70 – 7.67 (m, 2H), 7.59 (dd, *J* = 6.6, 3.9 Hz, 1H), 7.55 – 7.51 (m, 2H), 6.97 (d, *J* = 9.0 Hz, 2H), 6.80 (d, *J* = 9.0 Hz, 2H), 3.66 (s, 3H). **^{13}C NMR** (126 MHz, DMSO-d_6) δ 157.01, 139.94, 133.16, 130.54, 129.58, 127.13, 123.93, 114.74, 55.60. **HRMS** (ESI) m/z: $[M+H]^+$ calculated for $C_{13}H_{13}NO_3S$: 264.0689; found:264.0687.

4-Nitro-N-phenylbenzenesulfonamide (4c)

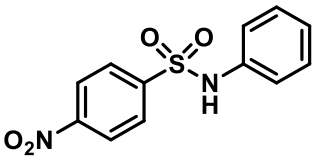

88% yield; yellow solid; m.p. 137-138°C; **^{1}H NMR** (500 MHz, DMSO-d_6) δ 8.23 (d, *J* = 8.7 Hz, 2H), 7.92 (d, *J* = 8.9 Hz, 2H), 6.99 (t, *J* = 7.3 Hz, 2H), 6.87 (d, *J* = 8.3 Hz, 2H), 6.63 (t, *J* = 7.2 Hz, 1H). **^{13}C NMR** (126 MHz, DMSO-d_6) δ 152.63, 148.44, 128.81, 128.03, 124.15, 121.31, 119.27. **HRMS** (ESI) m/z: $[M+H]^+$ calculated for $C_{12}H_{10}N_2O_4S$: 279.0434; found:279.0436.

4-Chloro-N-phenylbenzenesulfonamide (4d)

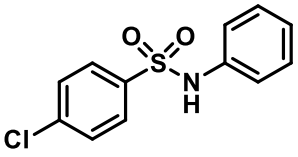

82% yield; white solid; m.p. 105-106°C; **^{1}H NMR** (500 MHz, DMSO-d_6) δ 7.76 (dd, *J* = 8.1, 1.4 Hz, 2H), 7.56 – 7.47 (m, 3H), 7.13 (t, *J* = 8.1 Hz, 1H), 7.02 (t, *J* = 2.0 Hz, 1H), 6.94 (d, *J* = 9.4 Hz, 1H), 6.87 (d, *J* = 7.9 Hz, 1H). **^{13}C NMR** (126 MHz, DMSO-d_6) δ 142.23, 133.54, 132.35, 130.82, 129.41, 126.92, 121.43, 119.60, 118.90. **HRMS** (ESI) m/z: $[M+H]^+$ calculated for $C_{12}H_{10}ClNO_2S$: 268.0194; found:268.0192.

4-Fluoro-N-(p-tolyl)benzenesulfonamide (4e)

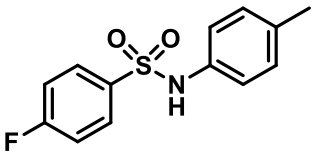

85% yield; white solid; m.p. 97-98°C; **^{1}H NMR** (500 MHz, DMSO-d_6) δ 10.15 (s, 1H), 7.60 (d, *J* = 8.3 Hz, 2H), 7.34 (d, *J* = 8.0 Hz, 2H), 7.08 (d, *J* = 6.8 Hz, 4H), 2.34 (s, 3H). **^{13}C NMR** (126 MHz, DMSO-d_6) δ 160.42, 158.50, 143.73, 136.85, 134.46, 130.13, 127.15, 123.16, 123.10, 116.39, 116.21, 21.41. **^{19}F NMR** (471 MHz, DMSO-d_6) δ -115.83. **HRMS** (ESI) m/z: $[M+H]^+$ calculated for $C_{13}H_{12}FNO_2S$: 266.0646; found:266.0648.

4-Trifluoromethyl-N-(p-tolyl)benzenesulfonamide (4f)

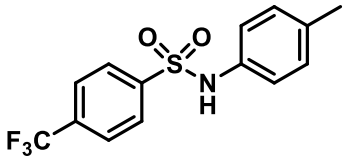

90% yield; white solid; m.p. 140-141°C; **^{1}H NMR** (500 MHz, DMSO-d_6) δ 10.82 (s, 1H), 7.72 (d, *J* = 8.3 Hz, 2H), 7.60 (d, *J* = 8.6 Hz, 2H), 7.37 (d, *J* = 8.1 Hz, 2H), 7.29 (d, *J* = 8.5 Hz, 2H), 2.34 (s, 3H). **^{13}C NMR** (126 MHz, DMSO-d_6) δ 144.22, 142.15, 136.81, 130.37, 127.27 – 126.63 (m), 119.11, 21.42. **^{19}F NMR** (471 MHz, DMSO-d_6) δ -60.47. **HRMS** (ESI) m/z: $[M+H]^+$ calculated for $C_{14}H_{15}NO_2S$: 262.0896; found:262.0893.

2-Methyl-N-phenylbenzenesulfonamide (4g)

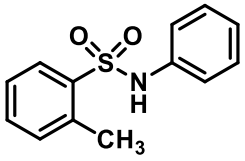

72% yield; white solid; m.p. 70-71°C; **^{1}H NMR** (500 MHz, DMSO-d_6) δ 9.57 (s, 1H), 7.66 (dd, *J* = 8.3, 1.2 Hz, 2H), 7.63 (d, *J* = 7.4 Hz, 1H), 7.55 (t, *J* = 7.6 Hz, 2H), 7.13 (dd, *J* = 5.5, 3.8 Hz, 1H), 7.09 (dd, *J* = 5.9, 3.4 Hz, 2H), 6.97 (dd, *J* = 5.5, 3.8 Hz, 1H), 1.98 (s, 3H). **^{13}C NMR** (126 MHz, DMSO-d_6) δ 141.06, 135.23, 134.63, 133.17, 131.19, 129.62, 126.98, 126.94, 126.78, 17.99. **HRMS** (ESI) m/z: $[M+H]^+$ calculated for $C_{13}H_{13}NO_2S$: 248.0740; found:248.0740.

2-Chloro-N-phenylbenzenesulfonamide (4h)

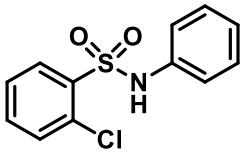

74% yield; white solid; m.p. 150-151°C; **^{1}H NMR** (500 MHz, DMSO-d_6) δ 7.75 – 7.72 (m, 2H), 7.56 – 7.52 (m, 1H), 7.52 – 7.48 (m, 2H), 7.18 (d, *J* = 8.8 Hz, 2H), 7.00 (d, *J* = 8.8 Hz, 2H). **^{13}C NMR** (126 MHz, DMSO-d_6) δ 132.39, 129.41, 129.18, 126.94, 122.11. **HRMS** (ESI) m/z: $[M+H]^+$ calculated for $C_{12}H_{10}ClNO_2S$: 268.0194; found:268.0196.

3-Chloro-N-phenylbenzenesulfonamide (4i)

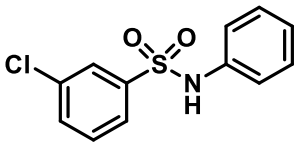

69% yield; white solid; m.p. 90-91°C; **^{1}H NMR** (500 MHz, DMSO-d_6) δ 10.88 (s, 1H), 8.00 – 7.96 (m, 2H), 7.88 – 7.83 (m, 2H), 7.82 (t, *J* = 7.5 Hz, 1H), 7.35 (d, *J* = 9.0 Hz, 2H), 7.14 (d, *J* = 8.9 Hz, 2H). **^{13}C NMR** (126 MHz, DMSO-d_6) δ 148.27, 136.08, 135.31, 133.13, 131.54, 130.37, 129.79, 129.38, 125.19, 122.59. **HRMS** (ESI) m/z: $[M+H]^+$ calculated for $C_{12}H_{10}ClNO_2S$: 268.0194; found:268.0196.

3-Nitro-N-phenylbenzenesulfonamide (4j)

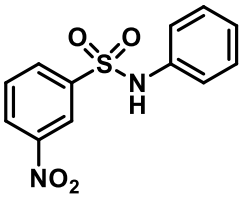

76% yield; orange solid; m.p. 110-111°C; **^{1}H NMR** (500 MHz, DMSO-d_6) δ 7.75 – 7.72 (m, 2H), 7.67 (s, 1H), 7.39 (dd, *J* = 4.6, 1.4 Hz, 3H), 7.32 (d, *J* = 7.6 Hz, 1H), 7.20 – 7.14 (m, 2H). **^{13}C NMR** (126 MHz, DMSO-d_6) δ 148.78, 146.19, 130.38, 129.39, 128.70, 127.47, 126.60, 113.63, 111.47. **HRMS** (ESI) m/z: $[M+H]^+$ calculated for $C_{12}H_{10}N_2O_4S$: 279.0434; found:279.0437.

2,4,6-Trimethyl-N-phenylbenzenesulfonamide (4k)

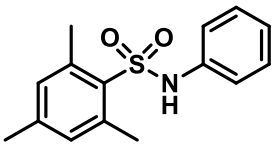

48% yield; white solid; m.p. 166-167°C; **^{1}H NMR** (500 MHz, DMSO-d_6) δ 10.16 (s, 1H), 7.21 (t, *J* = 7.9 Hz, 2H), 6.98 (dd, *J* = 8.7, 7.9 Hz, 5H), 2.55 (s, 6H), 2.22 (s, 3H). **^{13}C NMR** (126 MHz, DMSO-d_6) δ 142.47, 139.09, 138.12, 134.34, 132.24, 129.59, 124.01, 119.61, 22.90, 20.83. **HRMS** (ESI) m/z: $[M+H]^+$ calculated for $C_{15}H_{17}NO_2S$: 276.1053; found:276.1055.

N-(*p*-tolyl)naphthalene-1-sulfonamide (4l)

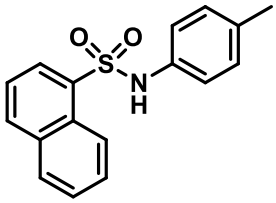

80% yield; white solid; m.p. 135-136°C; **^{1}H NMR** (500 MHz, DMSO-d_6) δ 8.05 (d, *J* = 8.8 Hz, 1H), 8.00 – 7.96 (m, 2H), 7.83 (d, *J* = 1.9 Hz, 1H), 7.62 – 7.56 (m, 2H), 7.49 (d, *J* = 8.0 Hz, 2H), 7.44 (dd, *J* = 8.7, 2.2 Hz, 1H), 7.13 (d, *J* = 7.8 Hz, 2H), 2.29 (s, 3H). **^{13}C NMR** (126 MHz, DMSO-d_6) δ 145.91, 138.28, 133.30, 132.07, 130.36, 128.58, 128.33, 128.02, 127.79, 127.00, 125.96, 121.56, 120.61, 21.24. **HRMS** (ESI) m/z: $[M+H]^+$ calculated for $C_{17}H_{15}NO_2S$: 298.0896; found:298.0894.

N-phenylpyridine-4-sulfonamide (4m)

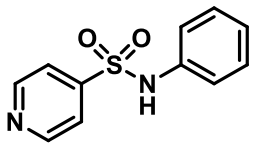

79% yield; white solid; m.p. 204-205°C; **^{1}H NMR** (500 MHz, DMSO-d_6) δ 7.75 (dd, *J* = 8.3, 1.3 Hz, 2H), 7.60 – 7.56 (m, 1H), 7.55 – 7.51 (m, 2H), 7.26 – 7.22 (m, 2H), 7.07 – 7.04 (m, 2H). **^{13}C NMR** (126 MHz, DMSO-d_6) δ 140.78, 138.93, 132.98, 129.61, 129.39, 127.43, 127.03, 122.11. **HRMS** (ESI) m/z: $[M+H]^+$ calculated for $C_{11}H_{10}N_2O_2S$: 235.0536; found:235.0538.

N-phenylthiazole-2-sulfonamide (4n)

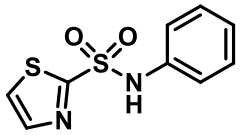

72% yield; white solid; m.p. 189-190°C; **^{1}H NMR** (500 MHz, DMSO-d_6) δ 7.83 – 7.79 (m, 2H), 7.61 – 7.57 (m, 1H), 7.56 – 7.52 (m, 2H), 7.26 (d, *J* = 4.6 Hz, 1H), 6.84 (d, *J* = 4.6 Hz, 1H). **^{13}C NMR** (126 MHz, DMSO-d_6) δ 142.8, 129.5, 126.3, 126.1, 124.9, 108.7. **HRMS** (ESI) m/z: $[M+H]^+$ calculated for $C_9H_9N_2O_2S_2$: 241.0100; found:241.0104.

N-phenylmethanesulfonamide (4o)

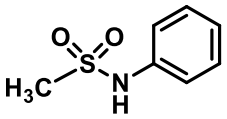

48% yield; white solid; m.p. 103-104ºC; **^{1}H NMR** (500 MHz, DMSO-d_6) δ 9.75 (s, 1H), 7.36 – 7.31 (m, 2H), 7.23 – 7.19 (m, 2H), 7.12 – 7.08 (m, 1H), 2.97 (s, 3H). **^{13}C NMR** (126 MHz, DMSO-d_6) δ 138.97, 129.75, 124.23, 120.25. **HRMS** (ESI) m/z: $[M+H]^+$ calculated for $C_7H_9NO_2S$: 172.0427; found:172.0425.

N-phenylbutane-1-sulfonamide (4p)

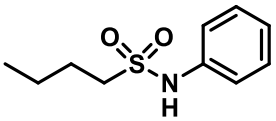

56% yield; white liquid; **^{1}H NMR** (500 MHz, DMSO-d_6) δ 7.79 (dd, *J* = 8.2, 1.4 Hz, 2H), 7.61 (dd, *J* = 10.7, 4.9 Hz, 3H), 2.72 (dd, *J* = 13.0, 7.0 Hz, 2H), 1.37 – 1.29 (m, 2H), 1.22 (dq, *J* = 14.1, 7.1 Hz, 2H), 0.79 (t, *J* = 7.3 Hz, 3H). **^{13}C NMR** (126 MHz, DMSO-d_6) δ 141.1, 132.8, 129.6, 127.0, 126.8, 42.7, 31.5, 19.6, 13.9. **HRMS** (ESI) m/z: $[M+H]^+$ calculated for $C_{10}H16NO_2S$: 214.0896; found:214.0894.

N-phenylcyclohexanesulfonamide (4q)

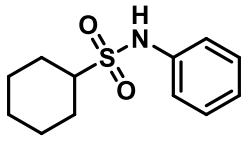

65% yield; white liquid; **^{1}H NMR** (500 MHz, DMSO-d_6) δ 7.83 – 7.80 (m, 2H), 7.65 (d, *J* = 7.4 Hz, 1H), 7.59 (ddd, *J* = 12.9, 5.9, 4.2 Hz, 3H), 2.92 (dd, *J* = 6.8, 3.4 Hz, 1H), 1.55 (dd, *J* = 8.0, 4.0 Hz, 4H), 1.43 (d, *J* = 12.0 Hz, 1H), 1.12 (dd, *J* = 19.5, 10.4 Hz, 5H). **^{13}C NMR** (126 MHz, DMSO-d_6) δ 142.7, 129.5, 126.8, 126.6, 52.6, 52.4, 33.7, 27.2, 24.7. **HRMS** (ESI) m/z: $[M+H]^+$ calculated for $C_{12}H_{18}NO_2S$: 240.1053; found:240.1051.

4-Aminobenzenesulfonamide (Sulphanilamide) (4r)

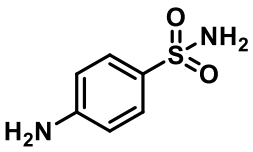

42% yield; white solid; m.p. 166-167°C; **^{1}H NMR** (500 MHz, DMSO-d_6) δ 7.45 (d, *J* = 8.7 Hz, 1H), 6.90 (s, 1H), 6.59 (d, *J* = 8.8 Hz, 1H), 5.82 (s, 1H). **^{13}C NMR** (126 MHz, DMSO-d_6) δ 152.38, 130.47, 127.89, 112.89. **HRMS** (ESI) m/z: $[M+H]^+$ calculated for $C_6H_8N_2O_2S$: 173.0379; found:173.0375.

4-Amino-N-(pyrimidin-2-yl)benzenesulfonamide (sulfadiazine) (4s)

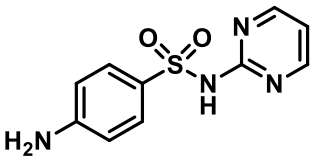

59% yield; white solid; m.p. 255-256°C; **^{1}H NMR** (500 MHz, DMSO-d_6) δ 11.26 (s, 1H), 8.48 (d, *J* = 4.8 Hz, 2H), 7.63 – 7.60 (m, 2H), 7.01 (t, *J* = 4.8 Hz, 1H), 6.58 – 6.55 (m, 2H), 6.01 (s, 2H). **^{13}C NMR** (126 MHz, DMSO-d_6) δ 158.72, 157.72, 153.49, 130.28, 125.37, 115.98, 112.59. **HRMS** (ESI) m/z: $[M+H]^+$ calculated for $C_{10}H_{10}N_4O_2S$: 251.0597; found:251.0594.

4-Amino-N-(6-methoxypyrimidin-4-yl)benzenesulfonamide (sulfamonomethozine) (4t)

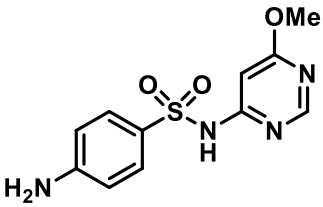

56% yield; white solid; m.p. 208-209°C; **^{1}H NMR** (500 MHz, DMSO-d_6) δ 11.38 (s, 1H), 8.39 (s, 1H), 7.55 (d, *J* = 8.8 Hz, 2H), 6.59 (d, *J* = 8.8 Hz, 2H), 6.31 (s, 1H), 6.11 (s, 2H), 3.83 (s, 3H). **^{13}C NMR** (126 MHz, DMSO-d_6) δ 170.24, 159.24, 157.93, 153.81, 129.67, 124.53, 113.00, 91.06, 54.36. **HRMS** (ESI) m/z: $[M+H]^+$ calculated for $C_{11}H_{12}N_4O_3S$: 281.0703; found:281.0706.

4-Amino-N-(5,6-dimethoxypyrimidin-4-yl)benzenesulfonamide (sulfadoxin) (4u)

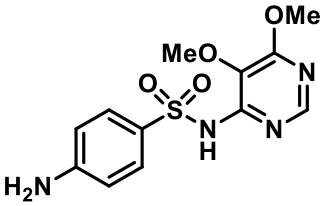

49% yield; white solid; m.p. 191-192°C; **^{1}H NMR** (500 MHz, DMSO-d_6) δ 10.63 (s, 1H), 8.12 (s, 1H), 7.63 (d, *J* = 8.8 Hz, 2H), 6.58 – 6.55 (m, 2H), 6.03 (s, 2H), 3.90 (s, 3H), 3.67 (s, 3H). **^{13}C NMR** (126 MHz, DMSO-d_6) δ 161.83, 153.52, 151.27, 151.04, 130.25, 127.17, 112.58, 60.64, 54.41. **HRMS** (ESI) m/z: $[M+H]^+$ calculated for $C_{12}H_{14}N_4O_4S$: 311.0809; found:311.0806.

4-Amino-N-(4,6-dimethylpyrimidin-2-yl)benzenesulfonamide (sulfamethazine) (4v)

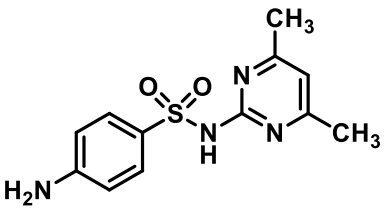

63% yield; white solid; m.p. 198-199°C; **^{1}H NMR** (500 MHz, DMSO-d_6) δ 11.02 (s, 1H), 7.64 (d, *J* = 8.8 Hz, 2H), 6.75 (s, 1H), 6.57 – 6.54 (m, 2H), 5.97 (s, 2H), 2.25 (s, 6H). **^{13}C NMR** (126 MHz, DMSO-d_6) δ 167.84, 157.12, 153.35, 130.77, 125.45, 114.31, 112.30, 23.58. **HRMS** (ESI) m/z: $[M+H]^+$ calculated for $C_{12}H_{14}N_4O_2S$: 279.0910; found:279.0914.

5.9 Spectra data of few compounds

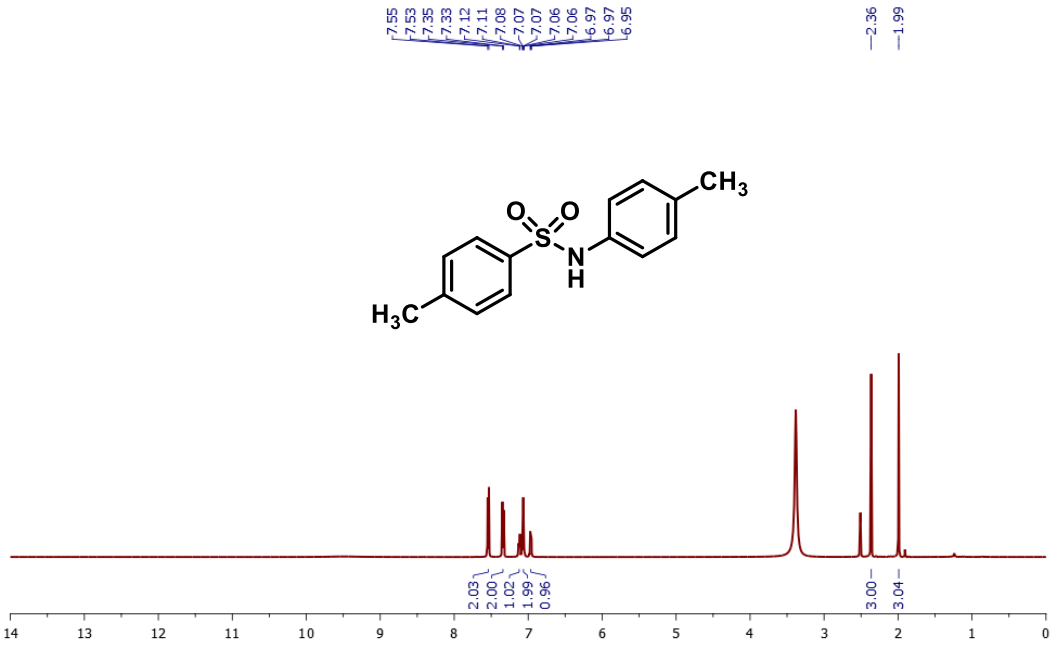

Figure 5.7 ^{1}H-NMR spectrum of **3a** (500 MHz, DMSO-d_6)

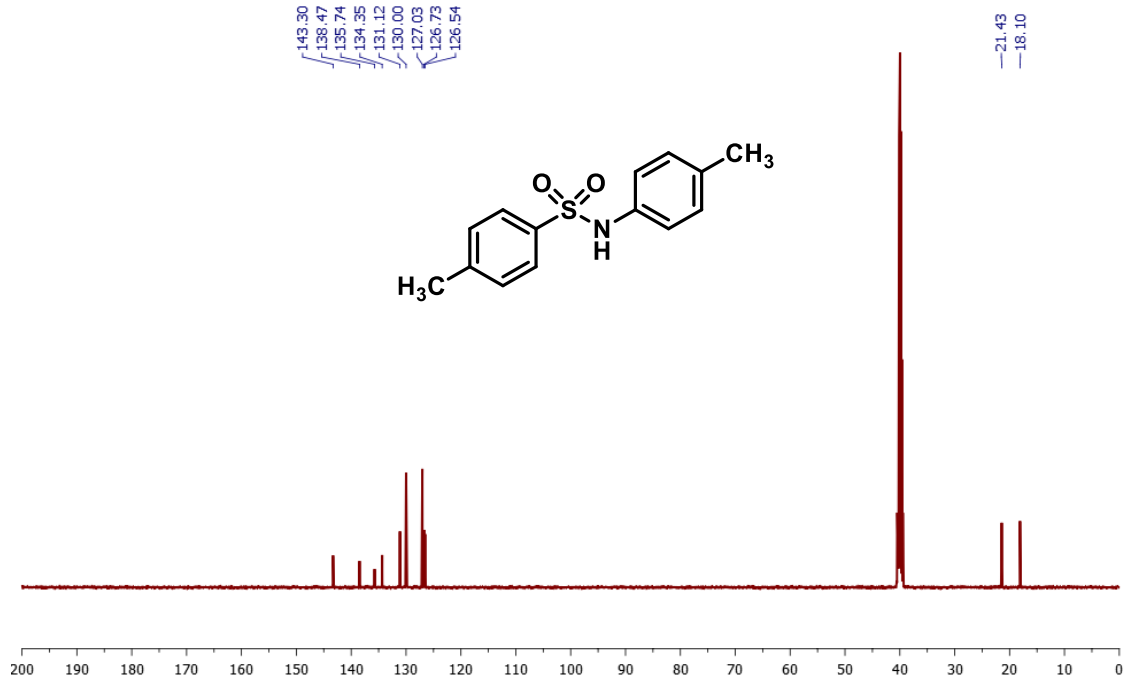

Figure 5.8 ^{13}C-NMR spectrum of **3a** (126 MHz, DMSO-d_6)

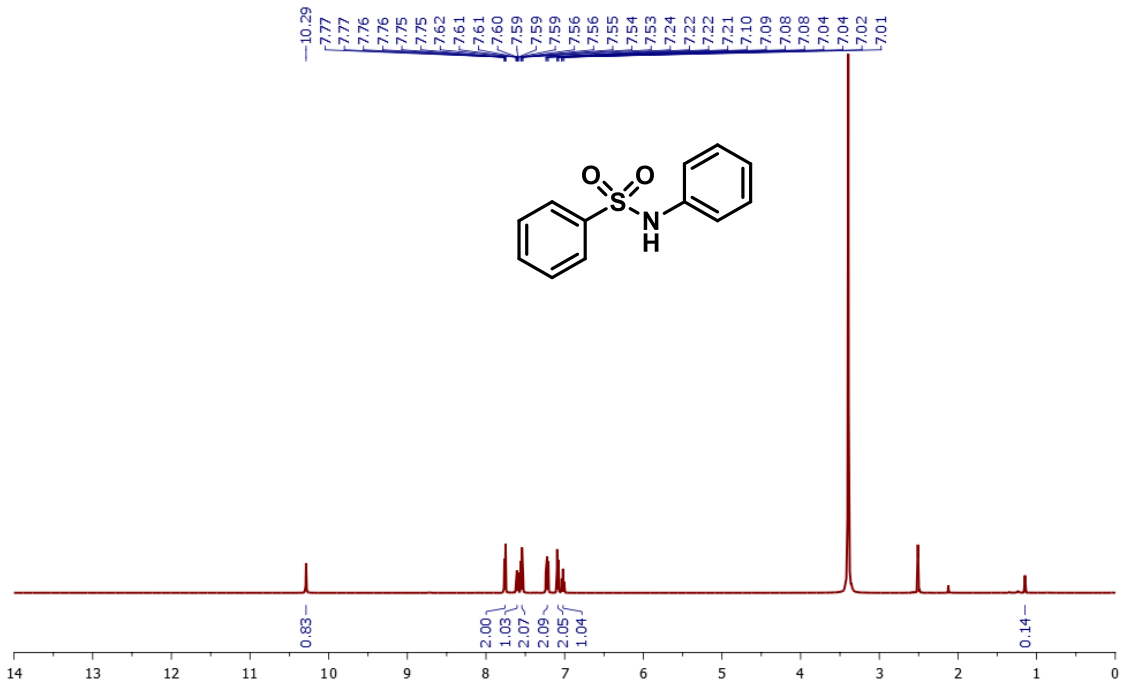

Figure 5.9 ^{1}H-NMR spectrum of **4a** (500 MHz, DMSO-d_6)

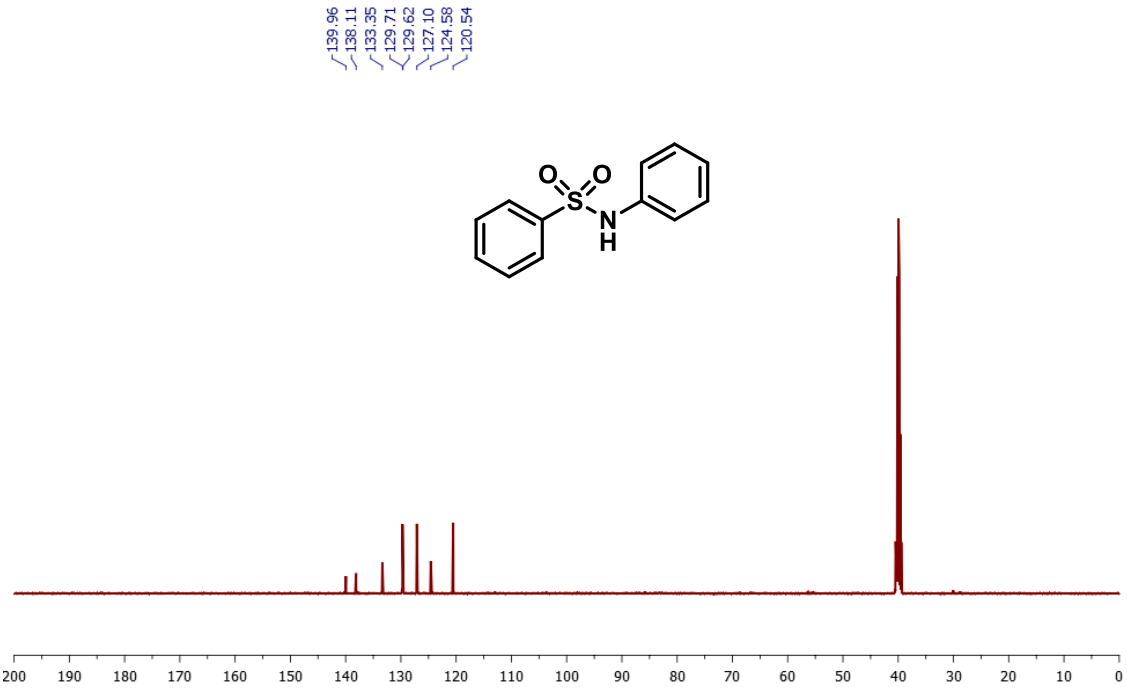

Figure 5.10 ^{13}C-NMR spectrum of **4a** (126 MHz, DMSO-d_6)

4.10 HRMS Data

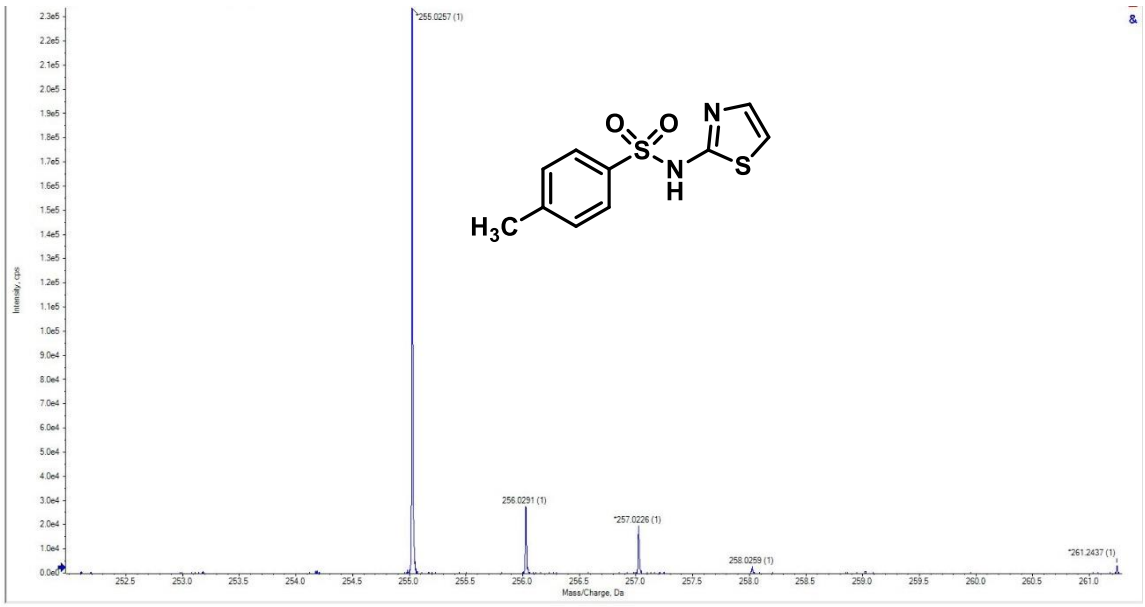

Figure 5.11 HRMS of compound **3o**

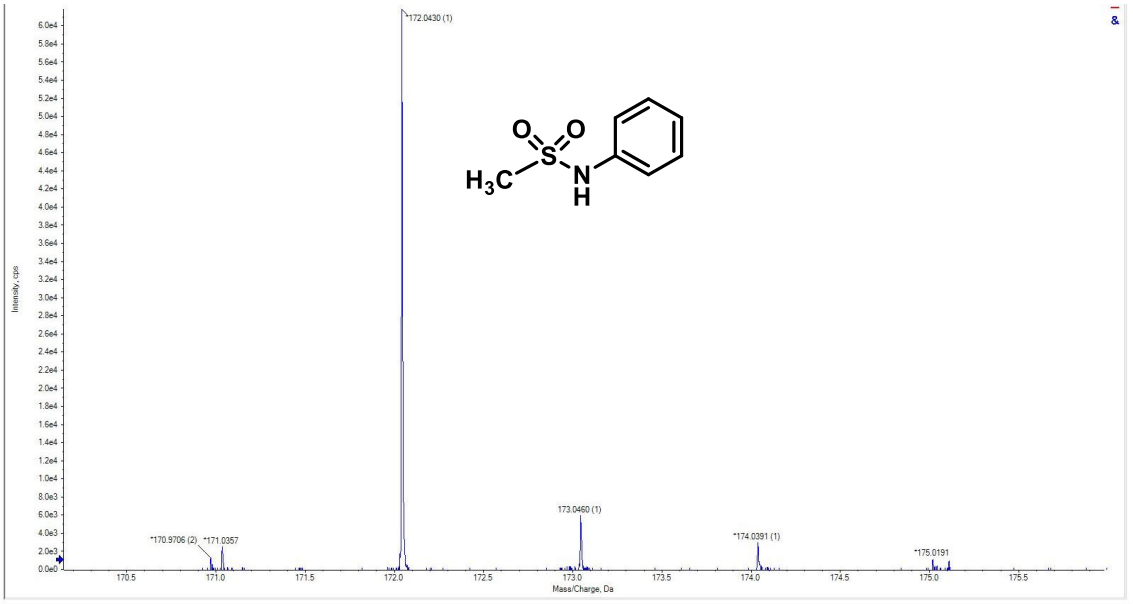

Figure 5.12 HRMS of compound **4n**

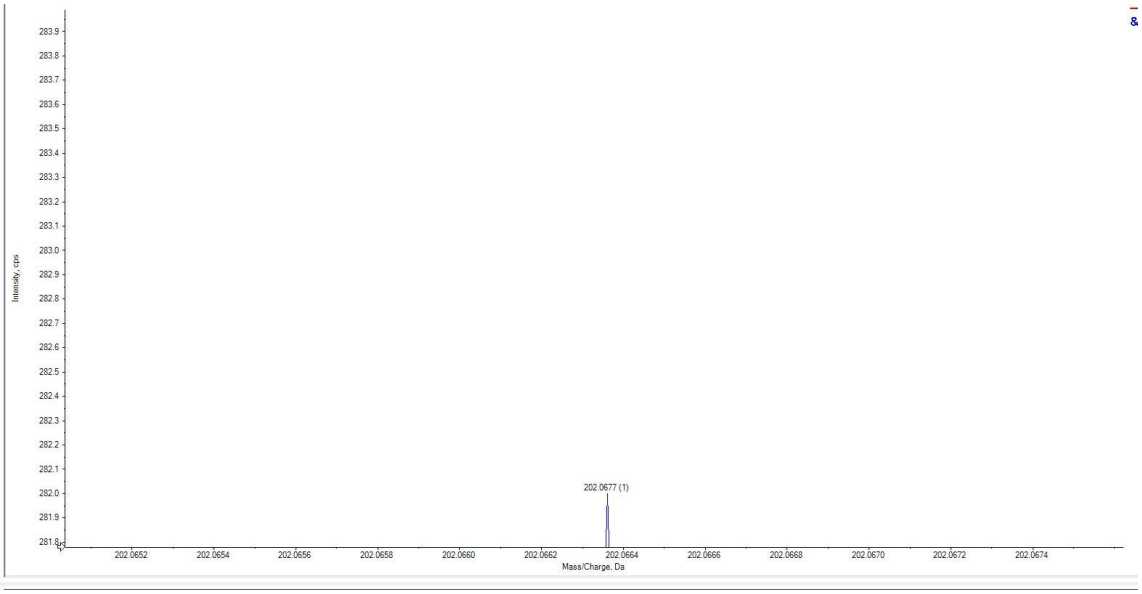

Figure 5.13 HRMS of intermediate **I**

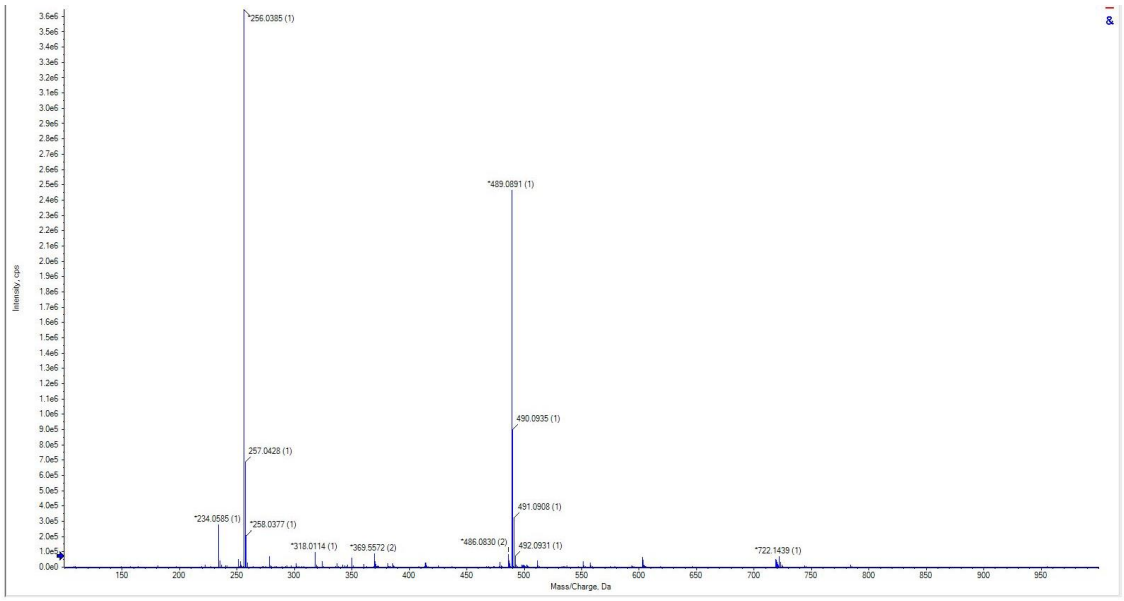

Figure 5.14 HRMS of the reaction mixture of H_2O^{18} labelling experiment

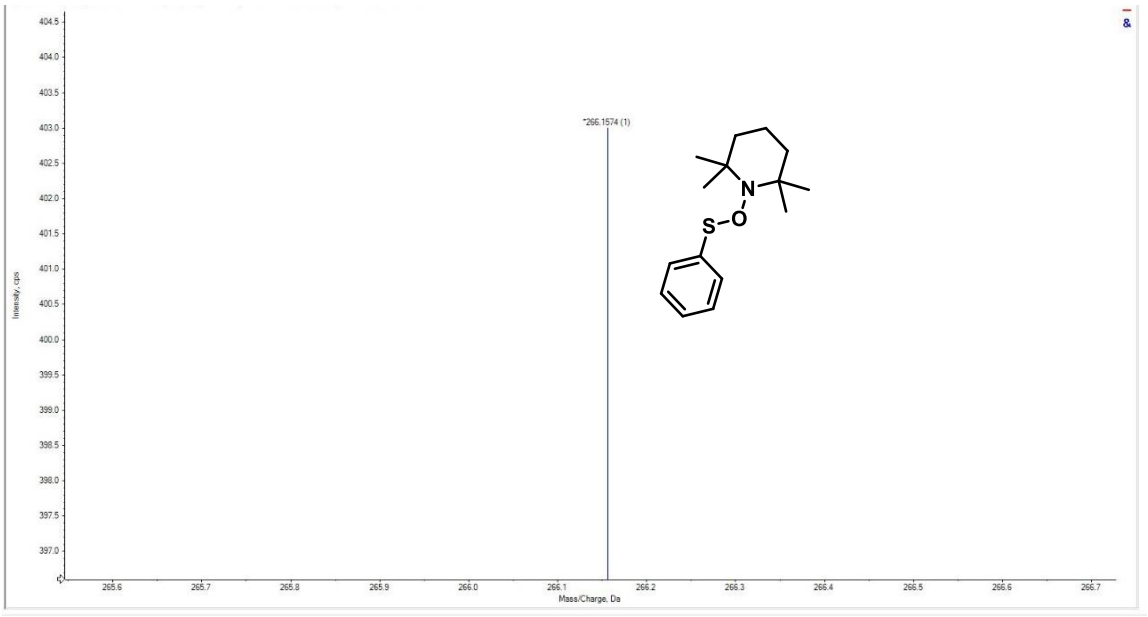

Figure 5.15 HRMS of adduct **5a**

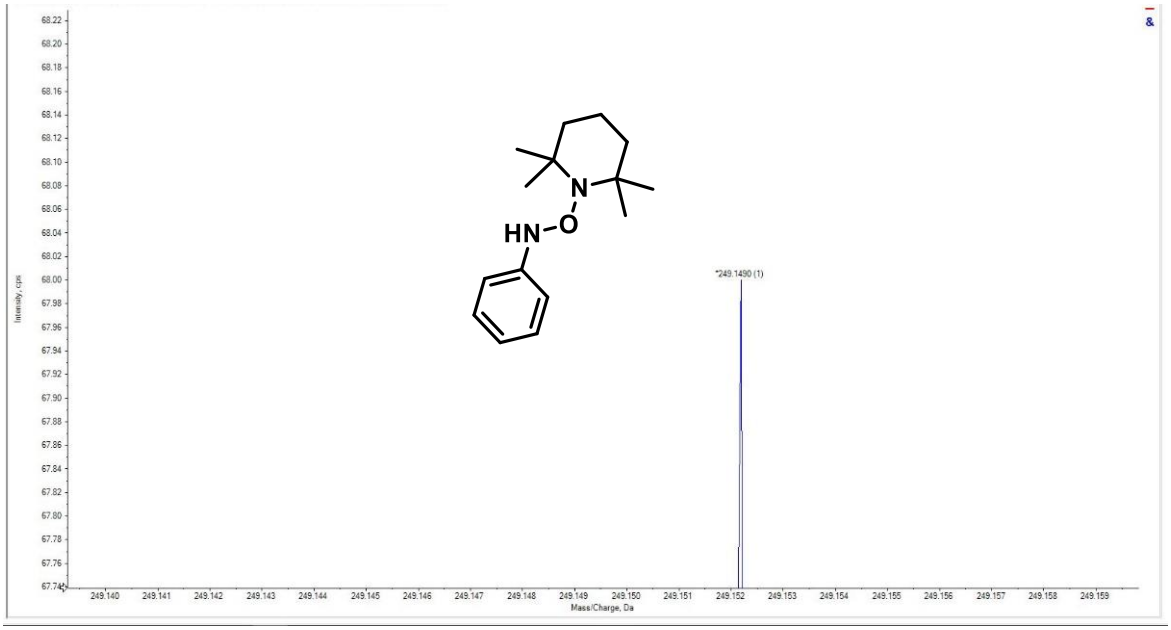

Figure 5.16 HRMS of adduct **6a**

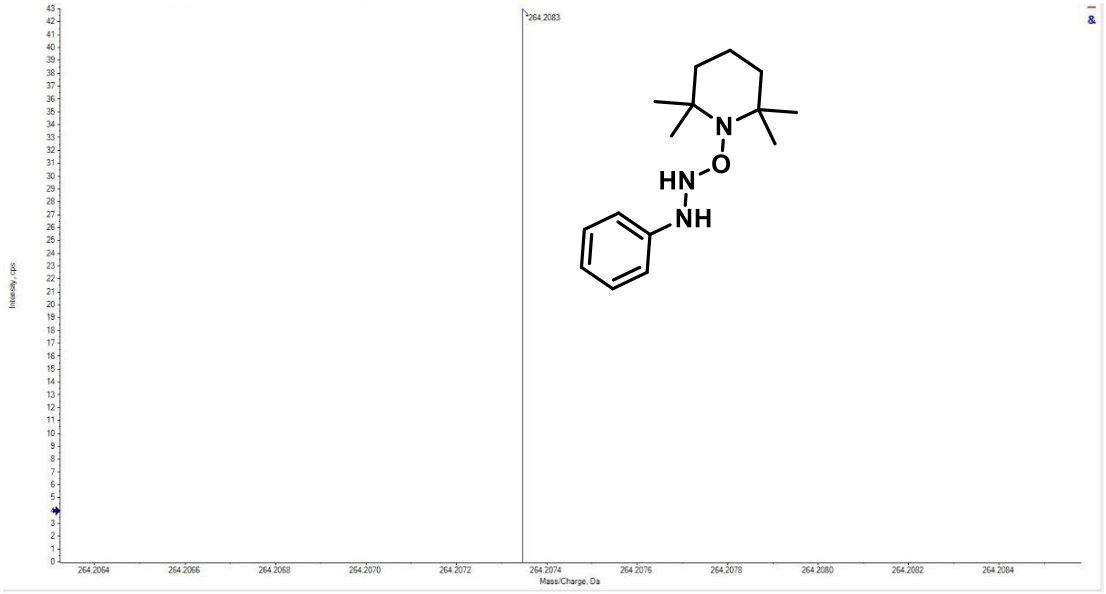

Figure 5.17 HRMS of adduct **7a**

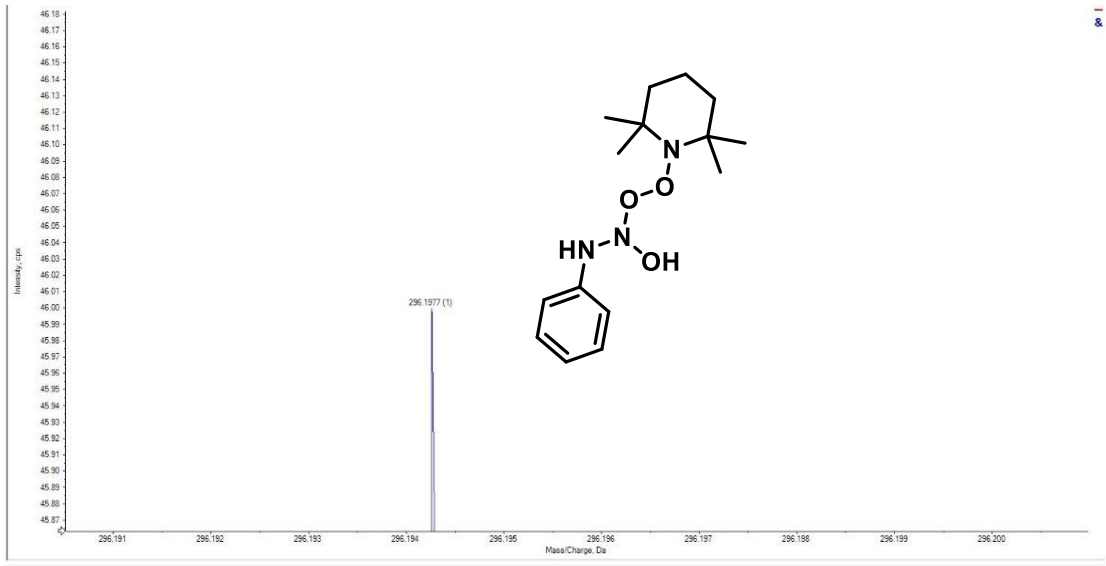

Figure 5.18 HRMS of adduct **8a**

5.11 References

[1] J.J. Petkowski, W. Bains, S. Seager, Natural products containing a nitrogen–sulfur bond, Journal of natural products, 81 (2018) 423-446.
[2] J. Drews, Drug discovery: a historical perspective, science, 287 (2000) 1960-1964.
[3] T. Zhu, Z. Lu, J. Fan, L. Wang, G. Zhu, Y. Wang, X. Li, K. Hong, P. Piyachaturawat, A. Chairoungdua, Ophiobolins from the mangrove fungus Aspergillus ustus, Journal of natural products, 81 (2018) 2-9.
[4] S. Apaydın, M. Török, Sulfonamide derivatives as multi-target agents for complex diseases, Bioorganic & medicinal chemistry letters, 29 (2019) 2042-2050.
[5] J.-F. Yang, M.-X. Chen, J.-H. Zhang, G.-F. Hao, G.-F. Yang, Genome-wide phylogenetic and structural analysis reveals the molecular evolution of the ABA receptor gene family, Journal of Experimental Botany, 71 (2020) 1322-1336.
[6] C.C. Hodges, G.J. De Boer, J. Avalos, Uptake and metabolism as mechanisms of selective herbicidal activity of the 1, 2, 4-triazolo [1, 5-a] pyrimidines, Pesticide Science, 29 (1990) 365-378.
[7] M. Wainwright, J.E. Kristiansen, On the 75th anniversary of Prontosil, Dyes and Pigments, 88 (2011) 231-234.
[8] S.K. Verma, R. Verma, F. Xue, P.K. Thakur, Y. Girish, K. Rakesh, Antibacterial activities of sulfonyl or sulfonamide containing heterocyclic derivatives and its structure-activity relationships (SAR) studies: A critical review, Bioorganic Chemistry, 105 (2020) 104400.
[9] S. Caddick, J.D. Wilden, D.B. Judd, Direct synthesis of sulfonamides and activated sulfonate esters from sulfonic acids, Journal of the American Chemical Society, 126 (2004) 1024-1025.
[10] O.M. Mulina, A.I. Ilovaisky, A.O. Terent'ev, Oxidative coupling with S–N bond formation, European Journal of Organic Chemistry, 2018 (2018) 4648-4672.
[11] D.C. Blakemore, P.M. Doyle, Y.M. Fobian, Synthetic Methods in Drug Discovery: Volume 1, Royal Society of Chemistry, 2016.
[12] K. Bahrami, M.M. Khodaei, M. Soheilizad, Direct conversion of thiols to sulfonyl chlorides and sulfonamides, The Journal of organic chemistry, 74 (2009) 9287-9291.
[13] A. Kołaczek, I. Fusiarz, J. Ławecka, D. Branowska, Biological activity and synthesis of sulfonamide derivatives: a brief review, Chemik, 68 (2014) 620-628.
[14] T.C. Das, S.A. Quadri, M. Farooqui, Recent advances in synthesis of sulfonamides: A review, Chemistry & Biology Interface, 8 (2018).
[15] N. Eid, I. Karamé, B. Andrioletti, Straightforward and sustainable synthesis of sulfonamides in water under mild conditions, European Journal of Organic Chemistry, 2018 (2018) 5016-5022.
[16] P.S. Pedersen, D.C. Blakemore, G.M. Chinigo, T. Knauber, D.W. MacMillan, One-Pot Synthesis of Sulfonamides from Unactivated Acids and Amines via Aromatic Decarboxylative Halosulfonylation, Journal of the American Chemical Society, 145 (2023) 21189-21196.

[17] R. Feng, Z.-Y. Li, Y.-J. Liu, Z.-B. Dong, Selective Synthesis of Sulfonamides and Sulfenamides from Sodium Sulfinates and Amines, The Journal of Organic Chemistry, 89 (2024) 1736-1747.
[18] T. Liu, D. Zheng, Z. Li, J. Wu, A Route to O-Aminosulfonates and Sulfonamides through Insertion of Sulfur Dioxide and Hydrogen Atom Transfer, Advanced Synthesis & Catalysis, 359 (2017) 2653-2659.
[19] Y. Chen, P.R. Murray, A.T. Davies, M.C. Willis, Direct copper-catalyzed three-component synthesis of sulfonamides, Journal of the American Chemical Society, 140 (2018) 8781-8787.
[20] M. Zhang, L. Liu, B. Wang, Y. Yang, Y. Liu, Z. Wang, Q. Wang, Direct Synthesis of Sulfonamides via Synergetic Photoredox and Copper Catalysis, ACS Catalysis, 13 (2023) 11580-11588.
[21] M. Wang, B.-C. Tang, J.-G. Wang, J.-C. Xiang, A.-Y. Guan, P.-P. Huang, W.-Y. Guo, Y.-D. Wu, A.-X. Wu, The triple role of rongalite in aminosulfonylation of aryldiazonium tetrafluoroborates: synthesis of N-aminosulfonamides via a radical coupling reaction, Chemical Communications, 54 (2018) 7641-7644.
[22] S.P. Blum, T. Karakaya, D. Schollmeyer, A. Klapars, S.R. Waldvogel, Metal-Free electrochemical synthesis of sulfonamides directly from (Hetero) arenes, SO_2, and Amines, Angewandte Chemie International Edition, 60 (2021) 5056-5062.
[23] Y. Cao, S. Abdolmohammadi, R. Ahmadi, A. Issakhov, A.G. Ebadi, E. Vessally, Direct synthesis of sulfenamides, sulfinamides, and sulfonamides from thiols and amines, RSC advances, 11 (2021) 32394-32407.
[24] H.-Y. Jang, Oxidative cross-coupling of thiols for S–X (X= S, N, O, P, and C) bond formation: mechanistic aspects, Organic & Biomolecular Chemistry, 19 (2021) 8656-8686.
[25] G. Laudadio, E. Barmpoutsis, C. Schotten, L. Struik, S. Govaerts, D.L. Browne, T. Noël, Sulfonamide synthesis through electrochemical oxidative coupling of amines and thiols, Journal of the American Chemical Society, 141 (2019) 5664-5668.
[26] Z. Bao, J. Zou, C. Mou, Z. Jin, S.-C. Ren, Y.R. Chi, Direct Reaction of Nitroarenes and Thiols via Photodriven Oxygen Atom Transfer for Access to Sulfonamides, Organic Letters, 24 (2022) 8907-8913.
[27] M. Zhu, N. Zheng, Photoinduced cleavage of N-N bonds of aromatic hydrazines and hydrazides by visible light, Synthesis, (2011) 2223-2236.
[28] K. Umehara, S. Kuwata, T. Ikariya, N–N Bond Cleavage of Hydrazines with a Multiproton-Responsive Pincer-Type Iron Complex, Journal of the American Chemical Society, 135 (2013) 6754-6757.
[29] L. Jia, Q. Tang, M. Luo, X. Zeng, Direct ortho-selective amination of 2-naphthol and its analogues with hydrazines, The Journal of Organic Chemistry, 83 (2018) 5082-5091.
[30] A. Gevorgyan, S. Mkrtchyan, T. Grigoryan, V.O. Iaroshenko, Application of Silicon-Initiated Water Splitting for the Reduction of Organic Substrates, ChemPlusChem, 83 (2018) 375-382.
[31] A. Humblot, L. Grimaud, A. Allavena, P.N. Amaniampong, K. De Oliveira Vigier, T. Chave, S. Streiff, F. Jérôme, Conversion of Ammonia to Hydrazine Induced by High-Frequency Ultrasound, Angewandte Chemie, 133 (2021) 25434-25438.

[32] Y. Kong, K. Wei, G. Yan, Radical coupling reactions of hydrazines via photochemical and electrochemical strategies, Organic Chemistry Frontiers, (2022).
[33] D. Singla, V. Luxami, K. Paul, Eosin Y mediated photo-catalytic C–H functionalization: C–C and C–S bond formation, Organic Chemistry Frontiers, 10 (2023) 237-266.
[34] G.-Q. Xu, P.-F. Xu, Visible light organic photoredox catalytic cascade reactions, Chemical Communications, 57 (2021) 12914-12935.
[35] Y. Lee, M.S. Kwon, Emerging organic photoredox catalysts for organic transformations, European Journal of Organic Chemistry, 2020 (2020) 6028-6043.
[36] A.K. Sahoo, D. Barik, B. Dam, B.K. Patel, Metal-Free Visible-light Mediated C− S Bond Formation, Asian Journal of Organic Chemistry, 12 (2023) e202300252.
[37] L. Marzo, S.K. Pagire, O. Reiser, B. König, Visible-light photocatalysis: does it make a difference in organic synthesis?, Angewandte Chemie International Edition, 57 (2018) 10034-10072.
[38] T. Patra, S. Mukherjee, J. Ma, F. Strieth-Kalthoff, F. Glorius, Visible-light-photosensitized aryl and alkyl decarboxylative functionalization reactions, Angewandte Chemie, 131 (2019) 10624-10630.
[39] M.H. Aukland, M. Šiaučiulis, A. West, G.J. Perry, D.J. Procter, Metal-free photoredox-catalysed formal C–H/C–H coupling of arenes enabled by interrupted Pummerer activation, Nature Catalysis, 3 (2020) 163-169.
[40] A. Kamal, V. Srivastava, S. Singh, Visible-light-induced arylation via an electron–donor–acceptor complex: a catalyst-free approach for the synthesis of N-(hetero) aryl sulfonamides, New Journal of Chemistry, 47 (2023) 14605-14609.
[41] H.K. Singh, A. Kamal, S. Kumari, S.K. Maury, A.K. Kushwaha, V. Srivastava, S. Singh, Visible-Light-Promoted Synthesis of Fusesd Imidazoheterocycle by Eosin Y under Metal-Free and Solvent-Free Conditions, ChemistrySelect, 6 (2021) 13982-13991.
[42] S.K. Maury, A.K. Kushwaha, A. Kamal, H.K. Singh, S. Singh, Visible light triggered synthesis of spiro [indoline-3, 4′-quinoline] via oxidative coupling of indole with enaminone and malononitrile, Journal of Molecular Structure, 1274 (2023) 134452.
[43] A.K. Kushwaha, S.K. Maury, A. Kamal, H.K. Singh, S. Pandey, S. Singh, Visible-light-absorbing C–N cross-coupling for the synthesis of hydrazones involving C (sp 2)–H/C (sp 3)–H functionalization, Chemical Communications, 59 (2023) 4075-4078.
[44] A. Kamal, H.K. Singh, S.K. Maury, A.K. Kushwaha, V. Srivastava, S. Singh, Photo-Triggered Synthesis of Sulfonamides in a Sustainable Solvent via Electron Donor-Acceptor Complex, Asian Journal of Organic Chemistry, 12 (2023) e202200632.
[45] S. Pandey, A. Kamal, A.K. Kushwaha, H.K. Singh, S.K. Maury, S. Singh, Photo-triggered C-arylation of active-methylene compounds with diazonium salts via an electron donor-acceptor (EDA) complex, Chemical Communications, 60 (2024) 1136-1139.
[46] A.K. Kushwaha, S.K. Maury, S. Kumari, A. Kamal, H.K. Singh, D. Kumar, Visible-Light-Initiated Oxidative Coupling of Indole and Active Methylene Compounds Using Eosin Y as a Photocatalyst, Synthesis, 54 (2022) 5099-5109.
[47] S. Khan, A.M. Nair, C.M. Volla, Visible-light mediated allylation of thiols with allylic alcohols, Organic Chemistry Frontiers, 10 (2023) 157-162.

[48] S. Balgotra, P.K. Verma, R.A. Vishwakarma, S.D. Sawant, Catalytic advances in direct functionalizations using arylated hydrazines as the building blocks, Catalysis Reviews, 62 (2020) 406-479.
[49] Y. Gao, H. Xu, S. Zhang, Y. Zhang, C. Tang, W. Fan, Visible-light photocatalytic aerobic oxidation of sulfides to sulfoxides with a perylene diimide photocatalyst, Organic & Biomolecular Chemistry, 17 (2019) 7144-7149.
[50] C. Ye, Y. Zhang, A. Ding, Y. Hu, H. Guo, Visible light sensitizer-catalyzed highly selective photo oxidation from thioethers into sulfoxides under aerobic condition, Scientific Reports, 8 (2018) 2205.